SS

Scopus Support (ELS) <ScopusSupport@elsevier.com>
To: A. Prasetyadi

Thu 3/21/2024 10:14 AM

Dear Andreas Prasetyadi,

Thank you for reaching us Scopus Support and my apology for the delayed response.

I understand that you trying to add some missing article via Scopus database.

For the article entitled "Development of a new fast drying determinant method using resistivity for the industry of coconut shell charcoal briquettes", I am happy to confirm that the journal and year in which the paper was published are covered in Scopus.

Please be aware that the indexation process generally takes several weeks for an article to be visible on Scopus, which may include acquisition, metadata processing and delivery.

We therefore encourage our customers to allow 6 more weeks after the publication date of the relevant article before it appears in the Scopus database.

Vol. 1 No. 8 (127) (2024): Energy-saving technologies and equipment
Published: 2024-02-29

Note: Once the document is reflected via Scopus database, it will automatically be added to each authors Scopus profile.

If you notice after 6 weeks that the article is yet to be added, please feel free contacting me and I'll be glad in assisting you again.

We are sorry for the inconvenience this has caused you.

Have a wonderful day and stay safe!

Kind regards,

Marc Montemayor
Customer Service Representative
ELSEVIER

Visit Elsevier Support Center

Eastern-European
JOURNAL
of Enterprise Technologies

Eastern-European Journal of Enterprise Technologies

Східно-Європейський
ЖУРНАЛ
передових технологій

▪ Energy-saving technologies and equipment

1/8 (127) 2024

Content

ENERGY-SAVING TECHNOLOGIES AND EQUIPMENT

The charcoal briquette industry faces the problem of the method for determining the drying stop during its production. The combustion method as the main method is time-consuming. The test needs 3 hours to get the result. In order to find a new fast method for drying determinant, the resistivity method was proposed for rainbow coconut shell charcoal briquettes. The briquettes had a length of 3.8 cm, height of 2.2 cm, and width of 2 cm with a half-tubular top side. 50 samples of each three drying conditions (wet, half-dry, and dry) of the same drying batch were collected. These conditions were determined by a drying expert of a coconut shell charcoal briquette company. Then, the resistances were measured and the geometrical factor was applied to find their resistivities. A model of resistivity in the cross-sectional layer was also applied to find the coefficients of front-tail, base-top, and side-side directions. These coefficients became a special way to find the position of the wet part in half-dry briquettes. The results of the work show that resistivities in combination with their distribution can potentially be used for fast drying stop determinant. The wet and dry briquettes have a resistivity difference order of 10^2. The resistivities of the wet and dry briquettes are 450 kiloohms and 28 megaohms for every centimeter of length, respectively. The half-dry and dry briquettes have the same order of resistivities. However, the resistivity distribution of both conditions is very different. The dry briquettes have homogenous resistivities among the measurements emphasizing the drying process of the solid. It was also found that the half-dry briquette has a surface dry part until 0.55 cm depth. The center of the briquette is still wet

Keywords: charcoal briquette, resistance measurement, fast drying determinant, resistivity method

UDC 661
DOI: 10.15587/1729-4061.2024.297541

DEVELOPMENT OF A NEW FAST DRYING DETERMINANT METHOD USING RESISTIVITY FOR THE INDUSTRY OF COCONUT SHELL CHARCOAL BRIQUETTES

Andreas Prasetyadi
Corresponding author
Doctor of Technical Sciences, Lecturer*
E-mail: pras@usd.ac.id
Rusdi Sambada
Doctor of Technical Sciences, Lecturer*
Petrus Kanisius Purwadi
Master of Technical Sciences, Lecturer*
*Department of Mechanical Engineering
Sanata Dharma University
Paingan, Maguwoharjo, Depok,
Sleman, Indonesia, 55282

Received date 21.11.2023
Accepted date 20.01.2024
Published date 28.02.2024

How to Cite: *Prasetyadi, A., Sambada, R., Purwadi, P. K. (2024). Development of a new fast drying determinant method using resistivity for the industry of coconut shell charcoal briquettes. Eastern-European Journal of Enterprise Technologies, 1 (8 (127)), 58–66. doi: https://doi.org/10.15587/1729-4061.2024.297541*

1. Introduction

Briquette is a kind of prospective solid fuel renewable energy for many parts of the world [1], therefore, its production has become important to study in recent years. The main reason for studying the topic is to find a method to provide affordable green energy. Charcoal briquette is considered a reasonable fuel for local communities especially the agricultural community [2]. Accordingly, local resources are becoming an important topic of discussion in the area [1]. Other popular issues are the technology and parameters for the production [3]. The charcoal briquette production consists of charcoal preparation, milling and mixing, compaction and molding, and drying.

Charcoal briquette drying is important in charcoal briquette production in terms of time, quality, and cost. Drying affects the moisture content of the briquette implying briquette quality [3, 4]. Excepting the charcoal processing, coconut shell charcoal briquette production needs 2/3 of the production time for drying in a plant applying a hot air oven. The drying time is far longer in the traditional method, which depends on simple solar drying. The intermittency of solar heat existance, temperature, and humidity variations during drying increase the drying time. Moreover, the time to move the briquette from the storage to the field where the briquettes are exposed to solar rays reduces the drying effectiveness. To reduce the drying time, a fossil fuel oven is usually applied. But this affects the drying cost and its carbon emission.

The drying time implies the cost of producing briquettes. Generally, it comes from the worker and production cycle. A longer drying time means a higher labor intensity. This also means higher investment costs to meet a specific amount productivity target. Some researchers reported that drying time determines the carbon content of the briquette. It implies the calorific values of the briquette, which is a primary quality parameter showing the quality of the briquette [5]. Therefore, drying time is an essential issue of charcoal briquette production. So, a study of fast drying determinant is relevant to conduct.

2. Literature review and problem statement

As renewable energy easily applied in many regions, charcoal briquette gets attention from many researchers, but its drying is rarely discussed. Some issues becoming the main topic of research include charcoal processing, briquette production steps and the availability of the material.

Charcoal briquettes can be produced from many organic material types, especially agriculture products. A briquette can be made from biomass waste or special wood planted for the briquette. Rice husk or straw, and palm shell or kernel, and sago are some waste that is used for briquettes. Rice husk or straw charcoal briquette can be produced with corn or cassava starch without any differences in its combustion characteristics [6]. The palm shell or kernel charcoal briquette was also reported to be a potential source of renewable energy in order to cope Ghana energy crisis [7]. The sago stem midrib can also be processed into an activated charcoal briquette [8]. Rubber wood waste for briquette production was reported as the added value of the plantation cycle [9]. As it comes from biomass, the charcoal briquette is regarded to have negative carbon emissions. Moreover, the biomass material of the briquette fuel is usually the secondary product or by-product of agriculture. Therefore, the emission goes for the main product. The emission is calculated from the processing only.

The briquette should have charcoal processing first. Temperature is important in charcoal processing and affects the final quality of solid fuel. Malaysian bamboos were made in a kiln at 750 °C to be charcoal suitable for domestic use [10]. Increasing temperature above 600 °C for charcoal processing of sapwood and heartwood increases fixed carbon, but reduces slightly the calorific value [11]. Below the temperature, higher temperature charcoal production increases the charcoal calorific value [12]. The effect of charcoal processing temperature on quality also appears in density, durability, compressive strength, and water resistance [13].

Other studies concerning charcoal briquette production are about briquette materials, binders, and quality tests. The availability of material is essential for briquette production concerning its sustainability and economic calculation [14]. The binder composition was studied for corn and cassava starch resulting in similar quality effects [15]. The same paper also mentioned the bonding relation to the hardness of the briquette. Compaction affected the calorific value positively, but it had a negative impact on the burning rate [16]. The quality is shown with proximity tests such as moisture, volatiles, ash, fixed carbon, and calorific values [17]. The quality of the briquette was also shown by combustion temperature and ignition rate. A good briquette was reported to have a high combustion temperature and low ignition rate [8, 16]. Research on the variability of quality was reported by [18]. The research mentions that a good quality briquette has high fixed carbon, heating value, and low ash and volatiles. The works show that drying is the only relatively homogenous parameter. The material becomes an issue due to the availability of local raw materials. The study's spirit is usually based on renewable energy necessity [7]. The bonding and composition are studied to meet optimum briquette production. However, the drying study in briquette production still needs to be explored.

The briquette drying issues are generally limited to moisture content and drying technology. A review on briquette production reported that 68 % of the briquette production concerned about moisture content. The moisture content of briquettes ranges from 2.50 % to 10.4 % [3]. However, targeting specific moisture in a production step is far from the research spotlight in pursuing briquette quality. The moisture content of the product generally becomes set for a certain process. The FAO receipt book for briquetting applies preheating before compacting rather than drying after compacting [19]. Preheating makes the briquette surface temperature being 200 °C when it leaves the compacting machine. Such temperature allows the drying process during cooling. However, the specific time for drying and its physicometric conditions were not provided. A different production method applying drying in an oven at 100 °C for 24 hours was reported to reach acceptable moisture content [9]. Both approaches focus on drying time not specific moisture target. This is in opposition to the production process of charcoal briquette in an enterprise, which needs moisture content as a target variable. The way to ensure the completion of the briquetting process has not been studied yet even despite many researches of briquettes reported. The lack of a drying stopping determinant method is the main issue of this research.

The drying process of solid materials, a typical process in industry, generally consists of three steps: constant rate, first fall, and second fall. First, a constant drying rate happens when the mass transfer exists to keep constant surface humidity. This condition takes place in a saturated system. The water is homogeneously distributed. The drop water content on the surface makes the water flow from the inner part to the surface. Second, the first drying rate fall is the main character of the process when the water content on the surface is below saturation. In this situation, the internal driving force cannot spontaneously flow the water to the surface. The drying process depends on surface contact with the air. Third, the second drying fall follows as the surface's water content is under the wet bulb condition. Temperature is vital to push water to the surface [20].

Drying a briquette, the process of reducing the water content and any other liquid-solid substances of a briquette, depends on relative humidity, temperature difference, contact surface and time. The main function of drying is to reduce the water content of a material [20]. The water content of a briquette affects its calorific value and some other quality parameters. In addition to temperature, humidity became the second important parameter affecting the results of drying in coating using water base material [21]. The temperature difference between the air and the material is also an essential parameter for the drying process [22]. A higher temperature of solids than that of air allows the water content to be released due to its internal driving force. Such drying is the main principle of the contact drying method. The temperature difference between the solid and the air affects the speed of water evaporation on the surface, which becomes the principle of the convective drying approach. A lower temperature of the solid also increases the evaporation speed following the diffusive and purging principle. Such phenomena are part of the hot-air drying method. The contact surface of the air and solid implies convective evaporation. Forced convective flow is usually applied to increase the evaporation rate. The more a briquette is exposed to air, the less water content is in the briquette.

Water content is hypothesized to be the reason for the increase in the electric conductivity of the briquette. Water insertion of compacted carbon particles increases its conductivity, especially in saturated conditions. The relationship between water and carbon is less significant than water – water [23]. The amount of water content in porous carbon still affects the conductivity due to ionic transport [24]. Water has a conductivity of $3.5\ 10^{-5}\ Sm^{-1}$, and amorphous carbon has a conductivity of $1.25\ 10^{3}\ Sm^{-1}$, but compaction of carbon reduces its conductivity without reducing its porosity [25]. The presence of water in the carbon-compacted block increases conductivity significantly.

The distribution of water inside the briquette during drying depends on evaporation on its surface. The process makes a distribution of water content inside inside the briquette. According to the report [22], water distribution follows the distance from the surface. The water content on the briquette surface is less water than in depth. The water content was left in the depth of the briquette. Separate dry and wet sections appear because of the drying steps. These sections create a pattern of resistivity. Therefore, the water content after the drying process of a briquette affects its resistivity. However, the study of the resistivity effects of the water content for briquette drying is scarce. With an assumption that the more water inside inside the briquette, the lower the electric resistance is, the model of the amount of water content can be traced through its resistivity. Higher electrical resistance happens when the briquette gets drier.

The drying process is essential in briquette production, and the study of briquette drying was out of the scope of research. The moisture content is generally considered as a given parameter. On the other hand, the industry is eager to get specific moisture content of the briquette. Accordingly, the resistivity is varied according to the water content of porous material. All this suggests conducting research on briquette drying to determine specific moisture as a target using briquette resistivity for indicating drying determinant.

3. The aim and objectives of the study

The aim of the study is to develop a fast determinant of charcoal briquette drying using the resistivity method on a rainbow coconut shell charcoal briquette.

To achieve the aim, the following objectives are accomplished:

– to ensure the states of the briquettes with measuring mass, density, burning rate, and comparing the normalized burning rate and density;

– to measure and average the electric resistance of the rainbow briquette in 3 different orientations; they are side to side, front to tail, and bottom to top;

– to calculate the resistivities of the briquettes according to a geometrical factor accommodating different shapes of surfaces;

– wet and dry model; to calculate the coefficients of the model and find the depth of the wet and dry part layer of the half-dry briquette.

4. Materials and methods

4. 1. Object and hypothesis of the study

This work tries to explore the possibility of applying resistivity for stop drying determinant using rainbow coconut shell charcoal briquettes. It is based on the hypothesis that the water content in a porous material affects the resistivity of the material. Therefore, different states of the briquette can be predicted through its resistivity. The resistivity is assumed to be homogenous in wet or dry conditions. To find the resistivity, the resistances of the briquette are measured. Modification according to the shape factor of the rainbow type is applied to find the resistivity.

An element's electric resistance depends on the material's length, cross-sectional area, and resistivity. Based on the principle, a model of the cross-sectional resistance ratio will be built assuming isotropic resistivity. The resistivity distribution will be applied to predict the water content of the material, indicating the drying process condition. The model will be plotted for resistances measured for wet, half-dry, and dry charcoal determined by an experienced quality control person of a briquette company as validation.

4. 2. Rainbow coconut shell charcoal briquette

The briquettes used in the study were rainbow-type coconut shell briquettes collected from a briquette company in Klaten, Central Java, Indonesia. They had a length of 3.8 cm, a height of 2.2 cm, and a width of 2 cm. Therefore, the briquettes had a volume of 11.4 cm^3. The base of the briquette is a rectangle, and the top of the briquette is half tube. The shape of the rainbow-type coconut shell charcoal briquette is shown in Fig. 1. The radius of the semi-tubular is half of the rectangle width.

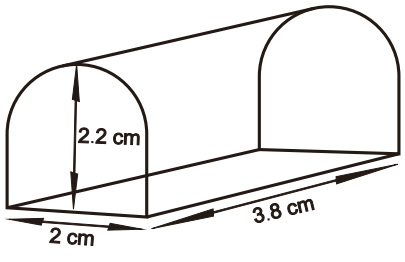

Fig. 1. Rainbow-type coconut shell charcoal briquette and its dimensions

The calorific value of the briquette is rated as 7,000 cal/gr. The briquette had a composition of 95 % coconut shell charcoal and 5 % starch of cassava flour. Thirty percent weight of demineralized water was added during mixing. Compaction with a ratio of 4:1 was conducted using a screw-type pressing machine during molding. Hot air drying was applied to the briquette for drying with an average temperature increase from room temperature to 100 °C in two days.

4. 3. Drying state model

The drying process follows the heat transfer and mass transfer principles. The water content removal as the mass transfer starts from the surface. It also happens to heat transfer. While the heat flows from the surface to the briquette's depth, there is a temperature gradient. The gradient forms a temperature contour shown in [21]. The contour also happens to the water content. The water content of the surface tends to be dryer than in depth. After the constant drying phase, the separation zone happens. There are two zones, dry and wet. Therefore, a wet and dry distribution model can be proposed for cross-section areas, as shown in Fig. 2. The wet and dry sections are distributed in horizontal and vertical cross-sections.

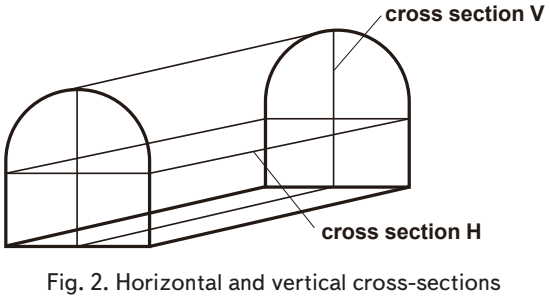

Fig. 2. Horizontal and vertical cross-sections

Assuming that the drying process in both cross-section areas is isotropic, the dry part of the cross-section is *b*. The wet part left in the center of the cross-section is signed with *a*. Additional alphabet after '*a*' shows part of the direction of the cross-section areas. *as* is used to name the wet part of the horizontal cross-section in the side-side direction. It is shown in Fig. 3. *ah* is applied for the wet part of the base-top direction in Fig. 4. *al* indicates the wet part in the front-tail direction as shown in Fig 5. It can be inferred that the horizontal cross-section has a wet part of *as* and *al*. The vertical cross-section has a wet part of *ah* and *al*.

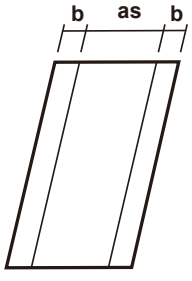

Fig. 3. Distribution of wet and dry parts in the side-side direction

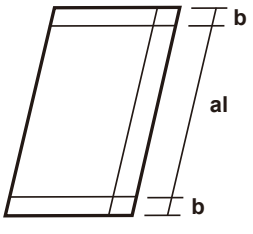

Fig. 4. Distribution of wet and dry parts in the front-tail direction

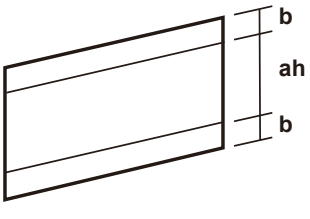

Fig. 5. Distribution of wet and dry parts in the base-top direction

Regarding the shape as mentioned in Fig. 1, only front and tail have equal distance for the cross-section. Therefore, the side-side layer needs adjustment of the cross-section area and the base-top layer needs adjustment of the distance. The cross-sections on opposite sides have the same distance. These adjustments become the geometrical factors.

4. 4. Resistance measurement

The resistance measurement of the briquettes was applied with two probes of digital ohmmeter with a sensitivity of 2 digits ranging from 0–40 megaohm. The resistance between the surfaces on opposite sides was measured on all surfaces of each briquette sample. There were 50 samples of each drying condition: wet, half-dry, and dry. The wet briquettes were the briquettes after leaving the compaction process and did not go for drying yet. Such briquettes have saturated water content. Half dry was the briquette having been in the oven for 1 of 2 days of drying. The temperature of the oven at that time was 50 °C. The dry briquettes were the briquettes leaving the oven under the QC inspection. The temperature of the oven when the drying stopped was 100 °C. The surface for the contact position of the probes and the probe distance are shown in Table 1.

Table 1

Resistance and probe position

Variable	Probe position	Probe distance (cm)
RL	Front and tail	3.8
RH	Base and top	2.2
RS	Left and right side	2

The positions of the probes as mentioned in Table 1 were on the longest distance of the cross-sections. With adjustment of the distance, the probe distance of the base-top became 1.985 cm. The distance was the average distance between the base and the top of the briquette.

4. 5. Analysis of resistance

Resistance is predicted to be proportional to the charcoal briquette length, resistivity, and its cross-section inverse. Even though the briquette has been compacted, it is still porous. In the briquette, the pores are filled with water. The water increases its conductivity. However, as the water is equally distributed through the briquette, the resistances R_L, R_H, and R_S are assumed to be proportional to each length and cross-section inverse. As the drying occurs, the resistance will increase following the reduction of the briquette's water-filled pores. Drying reduces the amount of water on the surface; therefore, the ratio of the water-filled porous part among the resistance direction will change as the briquette gets dryer.

The resistivity of the briquette is assumed to be equal and depends only on the water filling the pores. This resistivity shows the character of the material. Following the strategy in geophysics, the resistivity of a material can be traced from a measurement as equation (1). R_e and R_{eApp} are the resistivity of the material and its measurement result or apparent resistivity. K is the geometric factor representing the material's geometrical approach:

$$R_e = KR_{eApp}. \quad (1)$$

The shape of the rainbow briquette needs cross-section adjustment of the measured resistance, namely the cross-section factor. The factors are calculated assuming that the cross-sections of the briquette are equal on the opposite sides where the probes are located. For the front-tail side, both cross-sections are equal; the cross-section factor is equal to its cross-section. The half-conic shape affects the cross-section for the base-top and right side-left side. The cross-section factors are calculated from equation (2):

$$cross-section\ factor = \frac{volume}{probe\ distance}. \quad (2)$$

The assumed resistivity of the briquette with any water content is homogenous. Then, the resistance between the front and tail (R_L) is proportional to its length coefficient (L) – as mentioned in equation (3):

$$R_L = LR_e. \quad (3)$$

A similar approach can be applied to the resistance of left and right (R_S), and base and top (R_H). They are proportional to the width coefficient (S) and height coefficient (H), respectively, as mentioned in equation (4) and (5):

$$R_S = SR_e, \tag{4}$$

$$R_H = HR_e. \tag{5}$$

The wet condition gives a primary ratio proportional to its length. It is 3.8:2.2:2. It shows the ratio L_W:H_W:S_W. The subscript W of the coefficient means the wet condition. The ratio L_{HD}:H_{HD}:S_{HD} and L_D:H_D:S_D parts of the wet briquette in each direction in half dry and dry condition, respectively. The relationships of each coefficient will be:

$$R_{SHD} = asS_W R_{eW} + 2bS_W R_{eD}, \tag{6}$$

$$R_{HHD} = ahH_W R_{eW} + 2bS_W R_{eD}, \tag{7}$$

and

$$R_{LHD} = alL_W R_{eW} + 2bS_W R_{eD}, \tag{8}$$

with R_{eW} and R_{eD} being the specific resistance of the element in the wet and dry condition, respectively. It is also assumed that the wet area is located bS_W from the surface. Applying the ratio at wet, we can get:

$$R_{HHD} = 1.1ahS_W R_{eW} + 2bS_W R_{eD}, \tag{9}$$

and

$$R_{LHD} = 1.9alS_W R_{eW} + 2bS_W R_{eD}. \tag{10}$$

Equations (6)–(10) show that all of the resistances are functions of the width of the briquette and the specific resistance of the wet and dry states. Eliminating the second terms can be done by interoperating those equations. This gives equations (11)–(13). They are:

$$R_{HHD} - R_{SHD} = (1.1ah - as)S_W R_{eW}, \tag{11}$$

$$R_{HHD} - R_{LHD} = (1.1ah - 1.9al)S_W R_{eW}, \tag{12}$$

and

$$R_{LHD} - R_{SHD} = (1.9ah - as)S_W R_{eW}. \tag{13}$$

(11)–(13) only have S_w and R_{eW} as the coefficient ratio of side-to-side length and wet briquette resistivity, respectively. The coefficient allows calculating the first terms of equations (6)–(8).

5. Development of drying determinant using resistivity

5. 1. Ensuring briquette states

5. 1. 1. Density, burning rate

Density is the main difference between wet, half-dry, and dry briquettes due to the water content difference. The water content in the wet briquette is higher than in the others. Therefore, its density is the highest. The half-dry one also has a slightly higher density than the dry briquette. The wet briquette has a density higher than 1.4 g/cm^3. The dry briquette has a density of 1.14 g/cm^3. Accordingly, more than 3 g of water evaporated during drying. This accounts for nearly 30 % of the mass.

The average mass and density of the different water content of the briquette can be seen in Table 2. The table shows that wet briquette has the highest density and burning rate. Oppositely, the dry briquette has the lowest density and burning rate. In addition to differences in mass and density, the burning rate of the briquette also depends on the water content. The wetter, the higher the burning rate is. The difference between wet and dry briquette burning rates is about 0.04–0.05 g/min. The number is around 30 % of the burning rate mass of the dry briquette. This confirms the mass difference between dry and wet briquettes. In addition, 30 % water content does not affects the carbon combustion of the briquette. But it will decrease the calorific values of the briquette. Some heat is used for evaporating water.

Table 2

Mass, burning rate, and density of the briquette in each condition

Condition	Average mass (g)	Burning rate (g/min)	Density (g/cm^3)
Wet	16.71	0.221	1.465
Half-dry	13.06	0.199	1.146
Dry	13.00	0.175	1.140

5. 1. 2. Comparing the normalized burning rate and density

Normalization of the density and burning rate is calculated from the density and burning rate of wet briquettes. The normalization of the densities and burning rates was conducted according to the density of wet briquettes. Therefore, both normalizations of wet briquettes are ones. The comparison of the burning rate normalization and the density normalization can be used to predict whether water is distributed equally in the half-dry briquette. The comparison of the normalized burning rate and density of the briquettes in every condition is shown in Fig. 6.

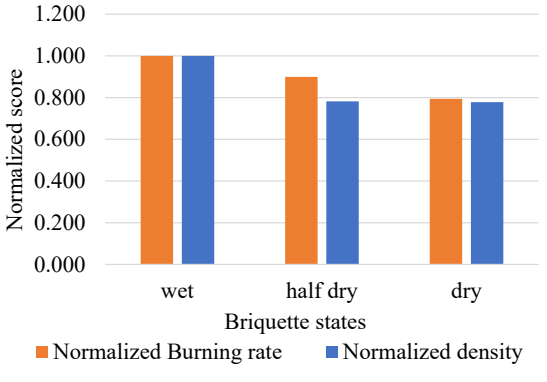

Fig. 6. Comparison of normalized burning rate and density

The half-dry briquette has the highest dissimilarity between the normalization of the burning rate and the normalization of the density. The wet briquette has equal normalizations of density and burning rate. The dry briquette has a slightly difference between the burning rate normalization and the density normalization. The half-dry briquette is

slightly different from the dry one, but it has a clear difference in burning rate. This means that water is not equally distributed in the half-dry briquette.

5. 2. Average resistance of rainbow briquettes

Table 3 mentions the average resistances of the wet, half-dry, and dry briquettes. *RL*, *RH*, and *RS* are the resistances of the front-tail direction, base-top direction, and side-side direction, respectively. *RL*s have the highest resistance among the other direction resistances. *RS*s tend to be the least resistances.

Table 3

Average resistances of wet, half-dry and dry condition

Condition	*RL*	*RH*	*RS*	Unit
BS (Wet)	151.1031	101.7528	63.1401	kOhm
SK (Half-Dry)	9.0814	6.62156	5.82362	MOhm
KR (Dry)	7.613911	6.198	5.32784	MOhm

Table 3 shows that generally, the resistance of the wet briquette is in kiloohms, while the resistances of other conditions are in units of megaohm. This indicates that the water content significantly affects the resistance. The water content increases the conductivity of the briquette. The length of the bands representing probe position distances affects its resistance. However, the resistance of dry conditions tends to be less than half dry in all conditions.

5. 3. Resistivities of briquettes

Applying the cross-section factor to the average resistance, the briquette resistivities for every centimeter and 1 cm of the square cross-section according to its direction are shown in Table 4. The cross-section factors of the briquette are shown in Table 5. The factors reflect the effects of the ends of the cross-section area where the probes are located.

Table 4

Resistivities of wet, half-dry and dry condition for every 1 cm^2 of the cross-section

Condition	*L*	*H*	*S*	Unit
RW	$5.698 \cdot 10^{-01}$	$4.694 \cdot 10^{-01}$	$3.204 \cdot 10^{-01}$	M·ohm·m
RHD	$3.424 \cdot 10^{1}$	$3.055 \cdot 10^{1}$	$2.955 \cdot 10^{1}$	M·ohm·m
RD	$2.871 \cdot 10^{1}$	$2.859 \cdot 10^{1}$	$2.704 \cdot 10^{1}$	M·ohm·m

Table 5

Cross-section factor of resistivity

Direction	Cross-section factor (cm^2)
L	3.771
H	4.613
S	5.074

The half-dry has the highest resistivity, but it has less homogeneous resistivity than the dry. This can be seen in Table 4. The element resistivity of 1 square centimeter briquette of the front-tail at half-dry was 3.424 10^{-1} M·ohm·m. But the left-right side resistivity of an element of 1 square centimeter was $2.955 \cdot 10^{-1}$ M·ohm·m. The dry briquette has $2.871 \cdot 10^{-1}$ M·ohm·m and $2.704 \cdot 10^{-1}$ M·ohm·m of the front-tail and side-side resistivity, respectively. The resistivity range of the half-dry briquette is 4.69 M·ohm·m, while the dry briquette has a resistivity range of 1.67 M·ohm·m.

Higher resistivity of the half-dry than dry briquette resistivity happens due to the character of the water content of the porous material. Amorphous carbon has higher conductivity than water. But the saturated water porous material allows ionic flows as aforementioned in the introduction. When the water was trapped inside the briquette, the cross-section of the briquette is smaller than that of the dry briquette. this implies higher resistivity of the half-dry briquette than that of the dry one. The range of resistivity also confirms the situation as the front-tail resistivity difference between half-dry and dry is higher than the side-side resistivity difference between both.

Averaging the resistivity in Table 4 informs the general resistivity of the briquette as shown in Table 6. The resistivity confirms that the wet briquette has much lower resistivity than half-dry and dry ones. The order of difference is 10^2. The wet briquette has a resistivity order of ten kilo ohm, while the half-dry or the dry briquette has a resistivity order of mega ohm. Therefore, it is easy to differentiate between the wet briquette and the half-dry or the dry briquette.

Table 6

Average resistivity of the briquette for 1 square centimeter

Condition	Resistivity (mega·ohm·m)	Standard deviation of resistivity (mega·ohm·m)
Wet	$5.196 \cdot 10^{-1}$	$1.254 \cdot 10^{-1}$
Half-dry	$3.240 \cdot 10^{1}$	2.472
Dry	$2.865 \cdot 10^{1}$	$9.340 \cdot 10^{-1}$

Applying equation (1) to the data of resistivity, the averages and their standard deviation can be found as shown in Table 6. The half-dry and the dry briquette have different resistivity distributions, even though they have the same order. Both have an order of mega ohm, but the half-dry standard deviation of the resistivity is 2.47 mega·ohm·m while the dry briquettes have a standard deviation of 0.93 mega·ohm·m. The dry briquette has less resistivity deviation than half-dry.

5. 4. Coefficients of the model and the depth of the wet part of the half-dry briquette

The resistivities given in Table 4 can be used for calculating equations (11), (12), and (13) to find –208.91, –7.1629, and –1.0983 for *ah*, *as*, and *al*, respectively. They are the coefficients of the model that can be used for calculating the position of the wet part of the half-dry briquette.

Application of the numbers to equation (5) can bring *b* as 0.553. The number means that 0.553 cm from the surface of the average half-dry briquette is dry while the rest is still wet. This is also confirmed by the work [26] explaining that after 5 hours of drying, the briquette surface was dry but the inside was damp. The rest of the briquette is still wet when the briquette is considered half-dry. In the dry briquette, this wet part disappears.

6. Discussion of the development of a fast drying determinant for the coconut shell charcoal briquette using resistivity

The dry briquette density of 1.14 g/cm^3 was very close to the average of the briquettes reviewed by [3]. The reviewed briquette densities ranged from 0.43–3.03 g/cm^3 with an average of 1.16 g/cm^3. This confirms the quality of the studied briquettes when they are dry.

The burning rate, mass and density as mentioned in Table 2 are proportional to each other. It can be interpreted that the heat was used to evaporate the wet briquette's water content. In other words, the burning rate is proportional to the fired fixed carbon and does not depend on water content. The wet briquette contains the largest amount of water, therefore it has the highest burning rate. For equal carbon combustion, the wet briquettes lost the highest amount of water.

The comparison of the normalized burning rate with the normalized density indicates that another essential factor took place for the half-dry briquette, as shown in Fig. 6, which is the water content location. The wet and dry briquettes have comparable normalized burning rates and density. However, the half-dry briquette has a significant difference in burning rate and density. The factor confirms the reason for the quality control people preferring to check the drying state using combustion rather than mass, even if the method needs a longer time to do. It can be inferred that a half-dry briquette relates to the combustion quality. The person does not focus on the density as the way to check because there is very little difference in density between half-dry and dry briquettes as shown in Fig. 6. The difference between the normalized burning rate and density trends in a half-dry briquette can be interpreted as the fact that the wet and dry parts exist separately in a half-dry briquette. The wet briquette has a relatively homogeneous water content among all of the briquettes. The dry briquette also has homogeneous conditions of being no water. The normalized density and normalized burning rate difference shows this homogeneity.

The difference of resistivity order can be easily used to determine the briquette that is not in wet condition. The distribution of resistivity data can be used to differentiate the half-dry and the dry briquette. The resistivities of the half-dry one tend to be spread, while the dry briquettes are homogenous. The difference of the half-dry briquettes can be in the order of 1 mega·ohm·m. The variation of the dry briquettes resistivities is less than 1 mega·ohm·m. Therefore, the strategy to check the stopping time of drying is as follows:

– collecting 10 briquettes randomly from the oven;

– measuring the resistances of each briquette in 3 directions;

– calculating the resistivities of the briquettes according to equation (1);

– if the resistivities < 1 mega·ohm·m, the briquettes are still wet;

– if the resistivities > 1 mega·ohm·m, check the standard deviations of the resistivities;

– if the standard deviation > 1 mega·ohm·m, the briquettes are still half-dry;

– if the standard deviation < 1 mega·ohm·m, the briquettes are dry. The drying process can be stopped. Otherwise, the oven has to be on for continuing the drying process.

The work can improve the decision time for charcoal briquette drying. The proposed approach does not need a combustion test. The normal combustion time for the briquette was 3 hours. However, some calculations are needed due to statistical calculation and logical decision procedure. Application development to help the operator can be done to make the method work easily. The operator just focuses on measuring the resistance of the briquettes.

In addition to the need to create an application to make the calculation easier, the method has the disadvantage of the necessity to collect randomly more than 10 briquettes from the oven. Opening the oven to collect the briquette for resistance measurement generally changes the condition of the oven. The temperature of the oven decreases and the humidity increases due to air flow from the outside. Accordingly, this affects the drying time. A skillful operator for collecting briquettes is important to limit the effect. This is also the reason for collecting briquettes in three conditions only rather than collecting drying time data.

The cross-sectional method provides information of the wet and dry parts model of rainbow briquettes. The coefficients earned from equations (11)–(13) can be used to find the location of the wet part from the surface. The wet part of average half-dry briquettes is located 0.553 cm from the surfaces. The dry part was on the surface until 0.553 cm. The wet part has a resistivity of 5.20 kiloohm·m. The dry part has a resistivity of 28 megaohm·m. The combination of the dry and wet parts of the briquette makes the bulk resistivity of the half-dry briquette higher than that of the dry briquette. The wet briquette has a lower resistivity than the dry one if the water content allows ions flowing across. In the case the wet part is enclaved inside the dry part, the ionic flow cannot exist. Therefore, the half-dry briquette seems to have a smaller cross-section than the dry briquette. Consequently, the half-dry briquette has a higher resistivity than the dry one.

The possibility to determine the location of the wet part enclaved inside the briquette is useful for other research on briquette drying. Different conditions of the briquettes provide different locations of the wet part. Small variations of the drying time difference can be conducted to understand more the mechanism of briquette drying. This will be useful to predict the optimal drying treatment of briquettes.

7. Conclusions

1. Three different briquette conditions were studied in terms of density, burning rate, and visual. The density of the wet briquettes was 1.4 g/cm^3. The dry coconut shell charcoal briquette density was 1.14 g/cm^3. The dry briquette is more porous than half-dry and wet, which can be seen using a microscope. The burning rates are also different. It is clear that there were three different conditions of the briquettes. Accordingly, the normalized densities were not linear to normalized densities. This indicates that the wet part was enclaved inside the half-dry briquette.

2. The wet rainbow briquette resistance has an order of kiloohm. The half-dry and dry briquette resistance has an order of megaohm. The clear difference of wet and dry indicates the possibility of applying the resistivities for drying stop determinant, especially to differentiate the wet and not wet.

3. The calculated average resistivities of the coconut shell charcoal briquette were 450 kiloohms, 3.1 megaohms, and 2.8 megaohms for the wet, half-dry, and dry briquette, respectively. The dry briquettes tend to be more homogenous in resistivity than half-dry briquettes. The dry briquette has less deviation than half-dry. This means that the resistivity distribution can be applied to differ the half-dry and dry briquettes.

4. The proposed cross-sectional model can inform the wet part of the half-dry briquette. With the coefficients of −208.91, −7.1629, and −1.0983 for the bottom-top, side-side, and front-tail wet part, it could be calculated that the half-dry briquette has the dry part just 0.553 cm from the surface. The other part inside the briquette is still wet.

While the resistivities can differ the wet from half-dry or dry briquette, the distribution of the resistivities can differ the dry from the half-dry briquette. Therefore, a combination of resistivities and their distribution can be applied for stopping drying as it can show the condition when the briquette is already dry. Practically, the briquette employee can use an ohmmeter to measure the briquette samples during the drying process. Such a process can be done faster than waiting for the conventional approach by a quality control person using a combustion test. In addition, the model can also show the position of the wet and dry parts of the half-dry briquettes.

Conflict of interest

The authors declare that the work does not have any conflict of interest.

Financing

The research is supported by DRTPM with contract number 181/E5/PG.02.00.PL/2023 and 0423.10/LL5-INT/AL.04/2023.

Data availability

The manuscript has data included as electronic supplementary material.

Use of artificial intelligence

The authors confirm that they did not use artificial intelligence technologies when creating the current work.

Acknowledgments

The authors express their gratitude to DRTPM for funding the research. They also appreciate Mr. Rony, Mr. Martono, Mr. Widodo, Mr. Intan for the support of the research activities.

References

1. Łaska, G., Ige, A. R. (2023). A Review: Assessment of Domestic Solid Fuel Sources in Nigeria. Energies, 16 (12), 4722. https://doi.org/10.3390/en16124722
2. Khan, A. U., Jan, Q. M. U., Abas, M., Muhammad, K., Ali, Q. M., Zimon, D. (2023). Utilization of Biowaste for Sustainable Production of Coal Briquettes. Energies, 16 (20), 7025. https://doi.org/10.3390/en16207025
3. Marreiro, H. M. P., Peruchi, R. S., Lopes, R. M. B. P., Andersen, S. L. F., Eliziário, S. A., Rotella Junior, P. (2021). Empirical Studies on Biomass Briquette Production: A Literature Review. Energies, 14 (24), 8320. https://doi.org/10.3390/en14248320
4. Sunardi, S., Djuanda, D., Mandra, M. A. S. (2019). Characteristics of Charcoal Briquettes from Agricultural Waste with Compaction Pressure and Particle Size Variation as Alternative Fuel. International Energy Journal, 19 (3), 139–148. Available at: http://www.rericjournal.ait.ac.th/index.php/reric/article/view/2199
5. Doloksaribu, M. (2014). Pembuatan Briket Arang Dari Tanah Gambut Pengganti Kayu Bakar. Jurnal Pengabdian kepada masyarakat Penerapan Ipteks, 20 (75), 70–77. Available at: https://www.researchgate.net/publication/314080916_Pembuatan_Briket_Arang_Dari_Tanah_Gambut_Pengganti_Kayu_Bakar
6. Adam, S. N. F. S., Aiman, J. H. M., Zainuddin, F., Hamdan, Y. (2021). Processing and Characterisation of Charcoal Briquettes Made from Waste Rice Straw as A Renewable Energy Alternative. Journal of Physics: Conference Series, 2080 (1), 012014. https://doi.org/10.1088/1742-6596/2080/1/012014
7. Osei Bonsu, B., Takase, M., Mantey, J. (2020). Preparation of charcoal briquette from palm kernel shells: case study in Ghana. Heliyon, 6 (10), e05266. https://doi.org/10.1016/j.heliyon.2020.e05266
8. Lestari, L., Variani, V. I., Firihu, Muh. Z., Raharjo, S., Saleh, I., Aprilla, N. (2020). Effect of Compaction Pressure on Quality of Activated Charcoal Briquette Made from Sago Stem Midrib Material. IOP Conference Series: Materials Science and Engineering, 797 (1), 012022. https://doi.org/10.1088/1757-899x/797/1/012022
9. Hamzah, F., Fajri, A., Harun, N., Pramana, A. (2023). Characterization of charcoal briquettes made from rubber rods and coconut shells with tapioca as an adhesive. IOP Conference Series: Earth and Environmental Science, 1182 (1), 012071. https://doi.org/10.1088/1755-1315/1182/1/012071
10. Jarawi, N., Jusoh, I. (2023). Charcoal properties of Malaysian bamboo charcoal carbonized at 750 °C. BioResources, 18 (3), 4413–4429. https://doi.org/10.15376/biores.18.3.4413-4429
11. Kwon, S.-M., Kwon, G.-J., Jang, J.-H., Kim, N.-H. (2012). Characteristics of Charcoal in Different Carbonization Temperatures. Journal of Forest and Environmental Science, 28 (4), 263–267. https://doi.org/10.7747/jfs.2012.28.4.263
12. Yan, W., Chen, Z., Sheng, K. (2015). Carbonization temperature and time improving quality of charcoal briquettes. Transactions of the Chinese Society of Agricultural Engineering, 31 (24), 245–249. doi: https://doi.org/10.11975/j.issn.1002-6819.2015.24.037
13. Saneewongnaayutaya, N., Khamdaeng, T., Panyoyai, N., Tippayawong, N., Wongsiriamnuay, T. (2022). Production and characterization of fuel briquettes from rice husks and tobacco stalks. AIP Conference Proceedings. https://doi.org/10.1063/5.0115139
14. Njenga, M. et al. (2021). Challenges and opportunities for charcoal briquette enterprises in East Africa. Available at: https://www.researchgate.net/publication/352561574_Challenges_and_opportunities_for_charcoal_briquette_enterprises_in_East_Africa

15. Adam, S. N. F. S., Zainuddin, F., Morgan, N. Z. S., Saroni, H. H. (2023). Comparison of Corn and Tapioca Starch Binders on the Characteristic of Rice Straw Charcoal Briquettes. Emerging Technologies for Future Sustainability, 59–69. https://doi.org/10.1007/978-981-99-1695-5_5
16. Pratama, B. H., Syarief, A., Saputra, M. R. P., Azis, A. P. (2022). Effect of Compaction Pressure and Sawdust Size on Briquette Made from Ulin Wood (Eusideroxylon Zwageri) and Gelam Wood (Melaleuca Cajuputi) to Combustion Characteristics. International Journal of Mechanical Engineering Technologies and Applications, 3 (2), 100. https://doi.org/10.21776/mechta.2022.003.02.4
17. Rapheal, I. A., Abayomi, B. (2021). Production and Characterisation of Briquettes from Maize Stalk and Neem Leaves Admixture. Acta Chemica Malaysia (ACMY), 5 (2), 77–81. Available at: https://www.actachemicamalaysia.com/acmy-02-2021-77-81/
18. Mencarelli, A., Cavalli, R., Greco, R. (2022). Variability on the energy properties of charcoal and charcoal briquettes for barbecue. Heliyon, 8 (8), e10052. https://doi.org/10.1016/j.heliyon.2022.e10052
19. Grover, P. D., Mishra, S. K. (1996). Biomass briquetting: Technology and Practices. Regional Wood Energy Development in Asia. Field Document No. 46. Food and Agriculture Organization of the United Nations. Bangkok. Available at: https://leehite.org/biomass/documents/Biomass%20Briquetting%20Technology%20and%20Practices%20FAO.pdf
20. Parikh, D. M. (2014). Solids Drying: Basics and Applications. Chemical Engineering, 42–45. Available at: https://www.researchgate.net/publication/283088778_Solids_Drying_Basics_and_Applications
21. Song, X., Wei, J., Mao, Z., Chi, X., Zhu, Z., Han, G., Cheng, W. (2023). Effect of Hot-Air Drying Conditions on the Drying Efficiency and Performance of a Waterborne Coating on Pine Wood. Forests, 14 (9), 1752. https://doi.org/10.3390/f14091752
22. Paul, G., Olivier, M., Esther, A., Daniel, M., Jean, C.-L. (2019). Heat and Mass Transfer Local Modelling Applied to Biomass Briquette Drying. Procedia Manufacturing, 35, 149–154. https://doi.org/10.1016/j.promfg.2019.05.018
23. Brennan, J. K., Bandosz, T. J., Thomson, K. T., Gubbins, K. E. (2001). Water in porous carbons. Colloids and Surfaces A: Physicochemical and Engineering Aspects, 187-188, 539–568. https://doi.org/10.1016/s0927-7757(01)00644-6
24. Rembert, F., Jougnot, D., Guarracino, L. (2020). A fractal model for the electrical conductivity of water-saturated porous media during mineral precipitation-dissolution processes. Advances in Water Resources, 145, 103742. https://doi.org/10.1016/j.advwatres.2020.103742
25. Ibrahim, M. H. I., Said, M. N., Asmawi, R. (2015). Characterization of Carbon Brush from Coconut Shell for Railway Application. Applied Mechanics and Materials, 773-774, 291–295. https://doi.org/10.4028/www.scientific.net/amm.773-774.291
26. Gunawan, S., Nursanni, B., Suprapto, Januariyansah, S. (2022). The utilization of biomass waste as charcoal briquette to reduce waste disposal. Journal of Physics: Conference Series, 2193 (1), 012086. https://doi.org/10.1088/1742-6596/2193/1/012086

ABSTRACT AND REFERENCES

ENERGY-SAVING TECHNOLOGIES AND EQUIPMENT

DOI: 10.15587/1729-4061.2024.298202

A COMPARATIVE ANALYSIS OF GAS-COOLED FAST REACTOR USING HETEROGENEOUS CORE CONFIGURATIONS WITH THREE AND FIVE FUEL VARIATIONS (p. 6–17)

Fajri Prasetya
University of Jember, Jawa Timur, Indonesia
ORCID: https://orcid.org/0009-0000-1760-4474

Ratna Dewi Syarifah
University of Jember, Jawa Timur, Indonesia
ORCID: https://orcid.org/0000-0001-9110-2093

Iklimatul Karomah
University of Jember, Jawa Timur, Indonesia
ORCID: https://orcid.org/0009-0003-0118-9044

Indarta Kuncoro Aji
PT. Kakiatna Indonesia and Phylion Battery Co. Ltd, South Jakarta Selatan, Indonesia
ORCID: https://orcid.org/0000-0002-6936-9178

Nuri Trianti
National Research and Innovation Agency, Jakarta, Indonesia
ORCID: https://orcid.org/0000-0001-6518-534X

GFR or Gas-cooled Fast Reactor is one type of fast generation-IV that uses a very high cooling temperature. Thus, it is necessary to have the right reactor core design so that the power distribution of neutrons produced reaches a safe and even limit point. The use of a uniform (homogeneous) reactor core can produce peaking power. This is very avoidable because it will cause a reactor accident. In this study, researchers tried to compare the results of the analysis for two heterogeneous reactor core designs including the configuration of 3 fuel variations and 5 fuel variations using UN-PuN fuel. This study aims to determine the k_{eff} value produced by both types of fuel variations during 5 years of burn-up and determine the characteristics of neutron flux, fission rate, and fission product during 15 years of burn-up. This study was started by calculating the homogeneous and heterogeneous core of 3 and 5 fuel variations with neutron transport simulation involving OpenMC. The calculation results show that the heterogeneous core configuration of 5 fuel variations for the k_{eff} value is more optimal than 3 fuel variations, because it has the smallest excess reactivity value. The neutron flux and fission rate characteristics for 5 fuel variations are more evenly distributed when compared to 3 fuel variations to maintain neutron lifetime and reactor life in operation. Burn-up residual plutonium material and minor actinide waste for 5 fuel variations have less mass than 3 fuel variations. The results of neutronic analysis of GFR reactors with heterogeneous reactor core designs for 5 fuel variations are better in terms of reactor criticality, neutron power distribution, and waste produced. Finally, optimization of the UN-PuN fuel volume fraction of 60 % provides the optimal k_{eff} value.

Keywords: comparative, fuel variations, Gas-cooled Fast Reactor, heterogeneous, k_{eff}, reactor core.

References

1. Syarifah, R. D., Sari, A. K., Arkundato, A., Irwanto, D., Su'ud, Z. (2022). Neutronics analysis of UN-PuN fuel for 300MW pressurized water reactor using SRAC-COREBN code. EUREKA: Physics and Engineering, 6, 12–23. https://doi.org/10.21303/2461-4262.2022.002247
2. Outlook Energi Indonesia 2021. Available at: https://www.slideshare.net/GbpGugun/bppt-outlook-energi-indonesia-2021pdf-260770253
3. Technology Roadmap Update for Generation IV Nuclear Energy Systems (2014). Gen IV International Forum. Available at: https://www.gen-4.org/gif/upload/docs/application/pdf/2014-03/gif-tru2014.pdf
4. Goldberg, S. M., Rosner, R. (2011). Nuclear Reactors: Generation to Generation. American Academy of Arts and Sciences. Available at: https://www.amacad.org/sites/default/files/academy/pdfs/nuclearReactors.pdf
5. Syarifah, R. D., Su'ud, Z., Basar, K., Irwanto, D., Pattipawaej, S. C., Ilham, M. (2017). WITHDRAWN: Comparison of uranium plutonium nitride (Usingle bondPusingle bondN) and thorium nitride (Thsingle bondN) fuel for 500 MWth Gas Cooled Fast Reactor (GFR) longlife without refueling. International Journal of Hydrogen Energy. https://doi.org/10.1016/j.ijhydene.2017.07.183
6. DOE Fundamentals Handbook Nuclear Physics and Reactor Theory. Volume 2 of 2 (1993). Department of Energy Washington DC. Available at: http://large.stanford.edu/courses/2014/ph241/alnoaimi2/docs/Nuclear-Volume2.pdf
7. Lestari, M. A., Fitriyani, D. (2014). Pengaruh Bahan Bakar UN-PuN, UC-PuC dan MOX terhadap Nilai Breeding Ratio pada Reaktor Pembiak Cepat. Jurnal Fisika Unand, 3 (1), 14–19. Available at: http://jfu.fmipa.unand.ac.id/index.php/jfu/article/view/60
8. Stainsby, R., Peers, K., Mitchell, C., Poette, C., Mikityuk, K., Somers, J. (2011). Gas cooled fast reactor research in Europe. Nuclear Engineering and Design, 241 (9), 3481–3489. https://doi.org/10.1016/j.nucengdes.2011.08.005
9. Dumaz, P., Allègre, P., Bassi, C., Cadiou, T., Conti, A., Garnier, J. C. et al. (2007). Gas-cooled fast reactors – Status of CEA preliminary design studies. Nuclear Engineering and Design, 237 (15-17), 1618–1627. https://doi.org/10.1016/j.nucengdes.2007.03.018
10. Raflis, H., Ilham, M., Su'ud, Z., Waris, A., Irwanto, D. (2021). Core Configuration Analysis for Modular Gas-cooled Fast Reactor (GFR) using OpenMC. Journal of Physics: Conference Series, 2072 (1), 012007. https://doi.org/10.1088/1742-6596/2072/1/012007
11. Syarifah, R. D., Yulianto, Y., Su'ud, Z., Basar, K., Irwanto, D. (2017). Neutronic Analysis of Thorium Nitride (Th, U^{233})N Fuel for 500MWth Gas Cooled Fast Reactor (GFR) Long Life without Refueling. Key Engineering Materials, 733, 47–50. https://doi.org/10.4028/www.scientific.net/kem.733.47
12. Ilham, M., Raflis, H., Suud, Z. (2021). Fuel Assembly Design Study for Modular Gas Cooled Fast Reactor using Monte Carlo Parallelization Method. Journal of Physics: Conference Series, 1772, 012025. https://doi.org/10.1088/1742-6596/1772/1/012025
13. Syarifah, R. D., Su'ud, Z., Basar, K., Irwanto, D. (2018). Neutronic Analysis of UN-PuN Fuel use FI-ITB-CHI Code for 500MWth GFR

Long Life Without Refueling. Journal of Physics: Conference Series, 1090, 012033. https://doi.org/10.1088/1742-6596/1090/1/012033

14. Syarifah, R. D., Aula, M. H., Arkundato, A., Nugroho, A. T. (2023). Design Study of 300 MWth GFR with UN-PuN Fuel using SRAC-COREBN Code. ARPN Journal of Engineering and Applied Science, 18 (4), 264–270. Available at: https://repository.unej.ac.id/jspui/bitstream/123456789/116091/1/MIPA_JURNAL_Design%20Study%20of%20300MWth%20GFR%20with%20UN-PuN%20Fuel%20using%20SRAC-COREBN%20Code.pdf
15. Novalianda, S. (2019). Power Flattening Desain Reaktor GFR Berbasis Bahan Bakar Uranium Plutonium Nitride (U, Pu)N. Journal of Electrical Technology, 4 (3), 140–143. Available at: https://jurnal.uisu.ac.id/index.php/jet/article/view/2070/1469
16. Dewi Syarifah, R., Su'ud, Z., Basar, K., Irwanto, D. (2017). Fuel Fraction Analysis of 500 MWth Gas Cooled Fast Reactor with Nitride (UN-PuN) Fuel without Refueling. Journal of Physics: Conference Series, 799, 012022. https://doi.org/10.1088/1742-6596/799/1/012022
17. Raflis, H., Ilham, M., Su'ud, Z., Waris, A., Irwanto, D. (2020). Neutronic Analysis of Modular Gas-cooled Fast Reactor for 5–25 % of Plutonium Fuel using Parallelization MCNP6 Code. Journal of Physics: Conference Series, 1493 (1), 012008. https://doi.org/10.1088/1742-6596/1493/1/012008
18. Karomah, I., Mabruri, A. M., Syarifah, R. D., Trianti, N. (2023). Analysis of core configuration for conceptual gas Cooled Fast Reactor (GFR) using OpenMC. Jurnal Teknologi Reaktor Nuklir Tri Dasa Mega, 25 (2), 85. https://doi.org/10.55981/tdm.2023.6879
19. The OpenMC Monte Carlo Code. OpenMC. Available at: https://docs.openmc.org/en/stable/
20. Romano, P. K., Horelik, N. E., Herman, B. R., Nelson, A. G., Forget, B., Smith, K. (2015). OpenMC: A state-of-the-art Monte Carlo code for research and development. Annals of Nuclear Energy, 82, 90–97. https://doi.org/10.1016/j.anucene.2014.07.048
21. Syarifah, R. D., Aula, M. H., Ardianingrum, A., Janah, L. N., Maulina, W. (2022). Comparison of thorium nitride and uranium nitride fuel on small modular pressurized water reactor in neutronic analysis using SRAC code. Eastern-European Journal of Enterprise Technologies, 2 (8 (116)), 21–28. https://doi.org/10.15587/1729-4061.2022.255849
22. Waltar, A. E., Reynalds, A. B. (1981). Fast Breeder Reactors. Pergamon Press. Available at: https://books.google.com.ua/books?hl=ru&lr=&id=4m6o1jMcIIIC&oi=fnd&pg=PR2&ots=cinb2vV2WU&sig=R8t2K0BrZ1oY5K4ek4-51xnOZzM&redir_esc=y#v=onepage&q&f=false
23. Advances in Small Modular Reactor Technology Developments (2018). IAEA. Available at: https://aris.iaea.org/Publications/SMR-Book_2018.pdf
24. Ilham, M., Raflis, H., Suud, Z. (2020). Full Core Optimization of Small Modular Gas-Cooled Fast Reactors Using OpenMC Program Code. Journal of Physics: Conference Series, 1493 (1), 012007. https://doi.org/10.1088/1742-6596/1493/1/012007
25. Raflis, H., Muhammad, I., Su'ud, Z., Waris, A., Irwanto, D. (2021). Reflector Materials Selection for Core Design of Modular Gas-cooled Fast Reactor using OpenMC Code. International Journal of Energy Research, 45 (8), 12071–12085. https://doi.org/10.1002/er.6042
26. Harsanti, D. (2010). Sintesis dan Karakterisasi Boron Karbida dari Asam Borat, Asam Sitrat dan Karbon Aktif. Jurnal Sains & Teknologi Modifikasi Cuaca, 11 (1), 29. https://doi.org/10.29122/jstmc.v11i1.2178
27. Mabruri, A. M., Syarifah, R. D., Aji, I. K., Hanifah, Z., Arkundato, A., Jatisukamto, G. (2022). Neutronic analysis on molten salt reactor FUJI-12 using 235U as fissile material in LiF-BeF2-UF4 fuel. Eastern-European Journal of Enterprise Technologies, 5 (8 (119)), 6–12. https://doi.org/10.15587/1729-4061.2022.265798
28. Pattipawaej, S. C., Su'ud, Z. (2018). Preliminary Study of Long-life GFR 100 and 150 MWth. Journal of Physics: Conference Series, 1090, 012073. https://doi.org/10.1088/1742-6596/1090/1/012073

DOI: 10.15587/1729-4061.2024.290996

NEUTRONIC DESIGN OF SMALL MODULAR LONG-LIFE PRESSURIZED WATER REACTOR USING THORIUM CARBIDE FUEL AT A POWER LEVEL OF 300–500 MWth·h (p. 18–27)

Boni Pahlanop Lapanporo
Institut Teknologi Bandung, Bandung, Indonesia
Universitas Tanjungpura, Pontianak, Indonesia
ORCID: https://orcid.org/0000-0002-0041-0427

Zaki Su'ud
Institut Teknologi Bandung; Nuclear Physics & Biophysics Research Division, Bandung, Indonesia
ORCID: https://orcid.org/0000-0001-8907-9824

Asril Pramutadi Andi Mustari
Institut Teknologi Bandung; Nuclear Physics & Biophysics Research Division, Bandung, Indonesia
ORCID: https://orcid.org/0000-0002-6546-4493

This study presents the neutronic design of a small modular long-life Pressurized Water Reactor (PWR) using thorium carbide fuel with ^{233}U fissile material. The target optimization for this study is a reactor designed to operate for 20 years, with excess reactivity throughout the reactor operational cycle consistently below 1.00 % dk/k. The analysis involves dividing the reactor core into three fuel regions with ^{233}U enrichment levels ranging from 3 % to 8 %, with a 1 % difference for each fuel region. To achieve optimum conditions, ^{231}Pa was randomly added to the fuel. The fuel volume fraction in this design varied from 30 % to 65 %, with a 5 % incremental variation. Power level variations are also studied within the 300–500 MWTH with increments of 50 MWTH. Calculations were performed using the Standard Reactor Analysis Code (SRAC) program with the PIJ and CITATION modules for cell and core calculations utilizing JENDL-4.0 nuclide data. Neutronic calculations indicate that the fuel with a 60 % volume fraction achieves optimum conditions at a power level of 300 MWTH. The best performance was observed with a fuel volume fraction of 65 %, reaching optimum conditions across power levels ranging from 300 to 500 MWTH. For the fuel with the best performance, the power density distributions for low and high power levels follow the same pattern radially and axially. The power peaking factor (PPF) for all fuel configurations

approaching the optimum conditions remains below two, a safe limit for the PWR. Other neutronic safety parameters, such as the Doppler coefficient and void fraction coefficient, also stay within the safe limits for the PWR, with both values remaining negative throughout the reactor operational cycle.

Keywords: thorium, core design, Doppler reactivity, void fraction coefficient, CITATION.

References

1. Nuclear Power in the World Today. Available at: https://world-nuclear.org/information-library/current-and-future-generation/nuclear-power-in-the-world-today.aspx
2. Cummins, W. E., Matzie, R. (2018). Design evolution of PWRs: Shippingport to generation III+. Progress in Nuclear Energy, 102, 9–37. https://doi.org/10.1016/j.pnucene.2017.08.008
3. Morales Pedraza, J. (2017). Small Modular Reactors for Electricity Generation. Springer International Publishing. https://doi.org/10.1007/978-3-319-52216-6
4. Mittag, S., Kliem, S. (2011). Burning plutonium and minimizing radioactive waste in existing PWRs. Annals of Nuclear Energy, 38 (1), 98–102. https://doi.org/10.1016/j.anucene.2010.08.012
5. Li, J., Li, X., Cai, J. (2021). Neutronic characteristics and feasibility analysis of micro-heterogeneous duplex ThO_2-UO_2 fuel pin in PWR. Nuclear Engineering and Design, 382, 111382. https://doi.org/10.1016/j.nucengdes.2021.111382
6. Galahom, A. A., Mohsen, M. Y. M., Amrani, N. (2022). Explore the possible advantages of using thorium-based fuel in a pressurized water reactor (PWR) Part 1: Neutronic analysis. Nuclear Engineering and Technology, 54 (1), 1–10. https://doi.org/10.1016/j.net.2021.07.019
7. Mirvakili, S. M., Alizadeh Kavafshary, M., Joze Vaziri, A. (2015). Comparison of neutronic behavior of UO_2, (Th-^{233}U)O_2 and (Th-^{235}U)O_2 fuels in a typical heavy water reactor. Nuclear Engineering and Technology, 47 (3), 315–322. https://doi.org/10.1016/j.net.2014.12.014
8. Baldova, D., Fridman, E., Shwageraus, E. (2014). High conversion Th-U^{233} fuel for current generation of PWRs: Part I – Assembly level analysis. Annals of Nuclear Energy, 73, 552–559. https://doi.org/10.1016/j.anucene.2014.05.017
9. Gorton, J. P., Collins, B. S., Nelson, A. T., Brown, N. R. (2019). Reactor performance and safety characteristics of ThN-UN fuel concepts in a PWR. Nuclear Engineering and Design, 355, 110317. https://doi.org/10.1016/j.nucengdes.2019.110317
10. Mohsen, M. Y. M., Abdel-Rahman, M. A. E., Galahom, A. A. (2021). Ensuring the possibility of using thorium as a fuel in a pressurized water reactor (PWR). Nuclear Science and Techniques, 32 (12). https://doi.org/10.1007/s41365-021-00981-0
11. Maiorino, J. R., Stefani, G. L., Moreira, J. M. L., Rossi, P. C. R., Santos, T. A. (2017). Feasibility to convert an advanced PWR from UO_2 to a mixed U/ThO_2 core – Part I: Parametric studies. Annals of Nuclear Energy, 102, 47–55. https://doi.org/10.1016/j.anucene.2016.12.010
12. Akbari-Jeyhouni, R., Rezaei Ochbelagh, D., Maiorino, J. R., D'Auria, F., Stefani, G. L. de (2018). The utilization of thorium in Small Modular Reactors – Part I: Neutronic assessment. Annals of Nuclear Energy, 120, 422–430. https://doi.org/10.1016/j.anucene.2018.06.013
13. Lau, C. W., Nylén, H., Demazière, C., Sandberg, U. (2014). Reducing axial offset and improving stability in PWRs by using uranium-thorium fuel. Progress in Nuclear Energy, 76, 137–147. https://doi.org/10.1016/j.pnucene.2014.05.016
14. Vaidyanathan, S. (2021). Transitioning to a Sustainable Thorium Fuel Cycle in Pressurized Water Reactors Using Bimetallic Thorium-Zirconium Alloy Cladding. Nuclear Technology, 207 (12), 1793–1809. https://doi.org/10.1080/00295450.2020.1846987
15. Peakman, A., Owen, H., Abram, T. (2021). Core design and fuel behaviour of a small modular pressurised water reactor using (Th, U)O_2 fuel for commercial marine propulsion. Progress in Nuclear Energy. https://doi.org/10.1016/j.pnucene.2021.103966
16. Subkhi, M. N., Su'ud, Z., Waris, A. (2013). Netronic Design of Small Long-Life PWR Using Thorium Cycle. Advanced Materials Research, 772, 524–529. https://doi.org/10.4028/www.scientific.net/amr.772.524
17. Syarifah, R. D., Aula, M. H., Ardianingrum, A., Janah, L. N., Maulina, W. (2022). Comparison of thorium nitride and uranium nitride fuel on small modular pressurized water reactor in neutronic analysis using SRAC code. Eastern-European Journal of Enterprise Technologies, 2 (8 (116)), 21–28. https://doi.org/10.15587/1729-4061.2022.255849
18. Kim, T. K., Grandy, C., Hill, R. N. (2009). Carbide and Nitride Fuels for Advanced Burner Reactor. International Conference on Fast Reactors and Related Fuel Cycles (FR09) - Challenges and Opportunities. Available at: https://inis.iaea.org/collection/NCLCollectionStore/_Public/41/070/41070109.pdf
19. Lapanporo, B. P., Su'ud, Z. (2022). Parametric Study of Thorium Fuel Utilization on Small Modular Pressurized Water Reactors (PWR). Journal of Physics: Conference Series, 2243 (1), 012062. https://doi.org/10.1088/1742-6596/2243/1/012062
20. Subki, I., Pramutadi, A., Rida, S. N. M., Su'ud, Z., Eka Sapta, R., Muh. Nurul, S. et al. (2008). The utilization of thorium for long-life small thermal reactors without on-site refueling. Progress in Nuclear Energy, 50 (2-6), 152–156. https://doi.org/10.1016/j.pnucene.2007.10.029
21. Dobuchi, N., Takeda, S., Kitada, T. (2016). Study on the relation between Doppler reactivity coefficient and resonance integrals of Thorium and Uranium in PWR fuels. Annals of Nuclear Energy, 90, 191–194. https://doi.org/10.1016/j.anucene.2015.11.018
22. Functional Design of Reactivity Control Systems. AP1000 Design Control Document. Available at: https://www.nrc.gov/docs/ML1117/ML11171A448.pdf

DOI: 10.15587/1729-4061.2024.298915

ENHANCING SAVONIUS ROTOR MODEL WITH ADDITIONAL GROOVES ON HYDROKINETIC TURBINE PERFORMANCE (p. 28–37)

Petrus Sampelawang
Hasanuddin University, South Sulawesi, Indonesia
Indonesian Christian Toraja University, South Sulawesi, Indonesia
ORCID: https://orcid.org/0000-0002-2166-8769

Nasaruddin Salam
Hasanuddin University, South Sulawesi, Indonesia
ORCID: https://orcid.org/0000-0003-4213-531X

Luther Sule
Hasanuddin University, South Sulawesi, Indonesia
ORCID: https://orcid.org/0000-0003-3384-6080

Rustan Tarakka
Hasanuddin University, South Sulawesi, Indonesia
ORCID: https://orcid.org/0000-0002-6083-650X

Hydrokinetic turbines use different rotors for technological and economic reasons. Even though it performs poorly, vertical-axis hydrokinetic turbines use the Savonius rotor. The object of research is a Savonius rotor model with additional grooves. The study addresses the need to improve the efficiency and overall performance of Savonius rotor models in hydrokinetic turbines, which are widely used for harnessing energy from flowing water currents. The problem involves understanding how different groove configurations affect the aerodynamic behavior and energy extraction efficiency of the Savonius rotor in hydrokinetic turbine applications. The test results revealed that incorporating grooves led to notable improvements in efficiency (η) and coefficient of drag (CD). Grooved blades exhibited a maximum efficiency of 30.97 % and a maximum drag coefficient of 2.71. Notably, blades with a groove width of 12.5 mm emerged as the optimal model, demonstrating an efficiency peak of 35.66 % and a drag coefficient 3.08. This indicates a substantial increase in efficiency by 4.69 % and a corresponding rise in the drag coefficient by 0.37 for grooved blades. The grooves on grooved blades increase friction, improving performance. Grooved rotor blades improve turbine performance significantly. Savonius rotor models in hydrokinetic turbines extract more energy by optimizing groove width and arrangement to maximize drag coefficient and efficiency. This research affects hydrokinetic turbine design and optimization for renewable energy generation. Engineers and designers can improve the performance and efficiency of the Savonius rotor model in hydrokinetic turbine applications by applying this study's findings.

Keywords: hydrokinetic turbine, Savonius rotor, grooved blade, drag coefficient, tip speed ratio.

References

1. Yuce, M. I., Muratoglu, A. (2015). Hydrokinetic energy conversion systems: A technology status review. Renewable and Sustainable Energy Reviews, 43, 72–82. https://doi.org/10.1016/j.rser.2014.10.037
2. Maldar, N. R., Ng, C. Y., Oguz, E. (2020). A review of the optimization studies for Savonius turbine considering hydrokinetic applications. Energy Conversion and Management, 226, 113495. https://doi.org/10.1016/j.enconman.2020.113495
3. Sule, L., Mochtar, A. A., Sutresman, O. (2020). Performance of Undershot Water Wheel with Bowl-shaped Blades Model. International Journal of Technology, 11 (2), 278. https://doi.org/10.14716/ijtech.v11i2.2465
4. Talukdar, P. K., Sardar, A., Kulkarni, V., Saha, U. K. (2018). Parametric analysis of model Savonius hydrokinetic turbines through experimental and computational investigations. Energy Conversion and Management, 158, 36–49. https://doi.org/10.1016/j.enconman.2017.12.011
5. Zhang, Y., Kang, C., Ji, Y., Li, Q. (2019). Experimental and numerical investigation of flow patterns and performance of a modified Savonius hydrokinetic rotor. Renewable Energy, 141, 1067–1079. https://doi.org/10.1016/j.renene.2019.04.071
6. Kumar, A., Saini, R. P. (2017). Performance analysis of a single stage modified Savonius hydrokinetic turbine having twisted blades. Renewable Energy, 113, 461–478. https://doi.org/10.1016/j.renene.2017.06.020
7. Basumatary, M., Biswas, A., Misra, R. D. (2018). CFD analysis of an innovative combined lift and drag (CLD) based modified Savonius water turbine. Energy Conversion and Management, 174, 72–87. https://doi.org/10.1016/j.enconman.2018.08.025
8. Alizadeh, H., Jahangir, M. H., Ghasempour, R. (2020). CFD-based improvement of Savonius type hydrokinetic turbine using optimized barrier at the low-speed flows. Ocean Engineering, 202, 107178. https://doi.org/10.1016/j.oceaneng.2020.107178
9. Sarma, N. K., Biswas, A., Misra, R. D. (2014). Experimental and computational evaluation of Savonius hydrokinetic turbine for low velocity condition with comparison to Savonius wind turbine at the same input power. Energy Conversion and Management, 83, 88–98. https://doi.org/10.1016/j.enconman.2014.03.070
10. Tian, W., Mao, Z., Ding, H. (2018). Design, test and numerical simulation of a low-speed horizontal axis hydrokinetic turbine. International Journal of Naval Architecture and Ocean Engineering, 10 (6), 782–793. https://doi.org/10.1016/j.ijnaoe.2017.10.006
11. Zahariev, M. E. (2016). Flow diagnostics and optimal design of vertical axis wind turbines for urban environments. University of Huddersfield. Available at: https://eprints.hud.ac.uk/id/eprint/31542/
12. Salam, N., Tarakka, R., Jalaluddin, Jimran, M. A., Ihsan, M. (2021). Flow Separation in Four Configurations of Three Tandem Minibus Models. International Journal of Mechanical Engineering and Robotics Research, 10 (5), 236–247. https://doi.org/10.18178/ijmerr.10.5.236-247
13. Torres, S., Marulanda, A., Montoya, M. F., Hernandez, C. (2022). Geometric design optimization of a Savonius wind turbine. Energy Conversion and Management, 262, 115679. https://doi.org/10.1016/j.enconman.2022.115679
14. Sharma, S., Sharma, R. K. (2016). Performance improvement of Savonius rotor using multiple quarter blades – A CFD investigation. Energy Conversion and Management, 127, 43–54. https://doi.org/10.1016/j.enconman.2016.08.087
15. Kerikous, E., Thévenin, D. (2019). Optimal shape of thick blades for a hydraulic Savonius turbine. Renewable Energy, 134, 629–638. https://doi.org/10.1016/j.renene.2018.11.037
16. Sodjavi, K., Ravelet, F., Bakir, F. (2018). Effects of axial rectangular groove on turbulent Taylor-Couette flow from analysis of experimental data. Experimental Thermal and Fluid Science, 97, 270–278. https://doi.org/10.1016/j.expthermflusci.2018.04.022
17. Kerikous, E., Thévenin, D. (2019). Performance Enhancement of a Hydraulic Savonius Turbine by Optimizing Overlap and Gap Ratios. Volume 2: Combustion, Fuels, and Emissions; Renewable Energy: Solar and Wind; Inlets and Exhausts; Emerging Technolo-

gies: Hybrid Electric Propulsion and Alternate Power Generation; GT Operation and Maintenance; Materials and Manufacturing (Including Coatings, Composites, CMCs, Additive Manufacturing); Analytics and Digital Solutions for Gas Turbines/Rotating Machinery. https://doi.org/10.1115/gtindia2019-2670

18. Soenoko, R., Purnami, P. (2019). Bowl bladed hydrokinetic turbine with additional steering blade numerical modeling. Eastern-European Journal of Enterprise Technologies, 4 (8 (100)), 24–36. https://doi.org/10.15587/1729-4061.2019.173986
19. Cengel, Y., Cimbala, J. (2013). Fluid mechanics fundamentals and applications. McGraw Hill, 1000.
20. Kini, C. R., Sharma, N. Y., Shenoy B., S. (2017). Fluid Structure Interaction Study of High Pressure Stage Gas Turbine Blade Having Grooved Cooling Channels. International Review of Mechanical Engineering (IREME), 11 (11), 825. https://doi.org/10.15866/ireme.v11i11.12465
21. Ahmadi-Baloutaki, M., Carriveau, R., Ting, D. S.-K. (2013). Effect of free-stream turbulence on flow characteristics over a transversely-grooved surface. Experimental Thermal and Fluid Science, 51, 56–70. https://doi.org/10.1016/j.expthermflusci.2013.07.001
22. Wan Yahaya, W. M. A., Samion, S., Mohd Zawawi, F., Musa, M. N., Najurudeen, M. N. A. (2020). The Evaluation of Drag and Lift Force of Groove Cylinder in Wind Tunnel. Journal of Advanced Research in Fluid Mechanics and Thermal Sciences, 68 (2), 41–50. https://doi.org/10.37934/arfmts.68.2.4150
23. Gowree, E. R., Jagadeesh, C., Atkin, C. J. (2019). Skin friction drag reduction over staggered three dimensional cavities. Aerospace Science and Technology, 84, 520–529. https://doi.org/10.1016/j.ast.2018.11.001
24. Seo, S.-H., Hong, C.-H. (2015). Performance improvement of airfoils for wind blade with the groove. International Journal of Green Energy, 13 (1), 34–39. https://doi.org/10.1080/15435075.2014.910777
25. Yao, J., Teo, C. J. (2022). Drag reduction by a superhydrophobic surface with longitudinal grooves: the effects of the rib surface curvature. Journal of Turbulence, 23 (8), 405–432. https://doi.org/10.1080/14685248.2022.2094936
26. Chehouri, A., Younes, R., Ilinca, A., Perron, J. (2015). Review of performance optimization techniques applied to wind turbines. Applied Energy, 142, 361–388. https://doi.org/10.1016/j.apenergy.2014.12.043

DOI: 10.15587/1729-4061.2024.298599

IDENTIFYING SOME REGULARITIES OF THE AERODYNAMICS AROUND WIND TURBINES WITH A VERTICAL AXIS OF ROTATION (p. 38–46)

Nazgul Tanasheva
Karaganda Buketov University, Karaganda, Republic of Kazakhstan
ORCID: https://orcid.org/0000-0003-4273-0960

Gulden Ranova
Karaganda Buketov University, Karaganda, Republic of Kazakhstan
ORCID: **https://orcid.org/0009-0006-9710-8406**

Amangeldy Satybaldin
Karaganda Buketov University, Karaganda, Republic of Kazakhstan
ORCID: https://orcid.org/0000-0002-0846-4665

Ainura Dyusembaeva
Karaganda Buketov University, Karaganda, Republic of Kazakhstan
ORCID: https://orcid.org/0000-0001-6627-7262

Asem Bakhtybekova
Karaganda Buketov University, Karaganda, Republic of Kazakhstan
ORCID: https://orcid.org/0000-0002-2018-8966

Nurgul Shuyushbayeva
Kokshetau University named after Sh. Ualikhanov, Kokshetau, Republic of Kazakhstan
ORCID: https://orcid.org/0000-0001-7166-6449

Sholpan Kyzdarbekova
Karaganda Buketov University, Karaganda, Republic of Kazakhstan
ORCID: https://orcid.org/0009-0000-9985-4636

Indira Sarzhanova
Karaganda Buketov University, Karaganda, Republic of Kazakhstan
ORCID: https://orcid.org/0009-0007-8053-6866

Nurgul Abdirova
Karaganda Buketov University, Karaganda, Republic of Kazakhstan
ORCID: https://orcid.org/0009-0005-1985-6081

The design of wind turbines with a vertical axis of rotation is quite simple, which successfully increases the level of efficiency. Existing vane wind turbines have a shortage of currents in the form of negative torque, and installations operating on the Magnus effect have a low lifting force. In this regard, the development and research of installations operating at speeds from 3 m/s, with combined blades with increased work efficiency is an urgent topic.

The object of the study is a wind turbine consisting of a system of rotating cylinders and fixed blades operating at low air flow speeds starting from 3 m/s. Numerical studies were carried out using the Ansys Fluent program and the implemented k-ε turbulence model. A special feature of the work is the combined use of two lifting forces: a cylinder and fixed blades, which made it possible to increase the output aerodynamic parameters. Calculations were performed for incoming flow rates of 3 m/s, 9 m/s, 15 m/s and cylinder rotation speeds of 315 rpm, 550 rpm, 720 rpm. It is determined that the period of change of the moment of forces T is 0.5 m/s, which corresponds to 2 revolutions of the wind wheel per minute. It was found that the cylinder rotation frequency in the range from 315 rpm to 720 rpm does not affect the period of change in the moment of forces, but the amplitude of the moment of forces increases with decreasing rotation frequency. The dependences of the rotation speed of the wind wheel on the velocity of the incoming flow, found by the method of sliding grids and 6DOF, are also obtained. It is determined that the installation begins to make revolutions from 3 m/s, with a positive torque of forces. The field of practical application of the numerical results will be useful for further research of wind turbines with combined blades.

Keywords: combined blade, fixed blade, Ansys-Fluent, moment of forces.

References

1. Elgendi, M., AlMallahi, M., Abdelkhalig, A., Selim, M. Y. E. (2023). A review of wind turbines in complex terrain. International Journal of Thermofluids, 17, 100289. https://doi.org/10.1016/j.ijft.2023.100289

2. Maheshwari, Z., Kengne, K., Bhat, O. (2023). A comprehensive review on wind turbine emulators. Renewable and Sustainable Energy Reviews, 180, 113297. https://doi.org/10.1016/j.rser.2023.113297
3. Kataray, T., Nitesh, B., Yarram, B., Sinha, S., Cuce, E., Shaik, S. et al. (2023). Integration of smart grid with renewable energy sources: Opportunities and challenges – A comprehensive review. Sustainable Energy Technologies and Assessments, 58, 103363. https://doi.org/10.1016/j.seta.2023.103363
4. Wilberforce, T., Olabi, A. G., Sayed, E. T., Alalmi, A. H., Abdelkareem, M. A. (2023). Wind turbine concepts for domestic wind power generation at low wind quality sites. Journal of Cleaner Production, 394, 136137. https://doi.org/10.1016/j.jclepro.2023.136137
5. Ganti, G., Gidden, M. J., Smith, C. J., Fyson, C., Nauels, A., Riahi, K., Schleußner, C.-F. (2023). Uncompensated claims to fair emission space risk putting Paris Agreement goals out of reach. Environmental Research Letters, 18 (2), 024040. https://doi.org/10.1088/1748-9326/acb502
6. Li, J., Peng, K., Wang, P., Zhang, N., Feng, K., Guan, D. et al. (2020). Critical Rare-Earth Elements Mismatch Global Wind-Power Ambitions. One Earth, 3(1), 116–125. https://doi.org/10.1016/j.oneear.2020.06.009
7. Global Wind Report 2022. Available at: https://gwec.net/global-wind-report-2022/
8. Liu, Z., Sing, J. J., Schwerdtfeger, P. (2023). Investigations of aerodynamics of three-bladed combined type wind turbine. Experimental and Theoretical NANOTECHNOLOGY, 171–180. https://doi.org/10.56053/7.1.171
9. Ahmad, M., Shahzad, A., Qadri, M. N. M. (2022). An overview of aerodynamic performance analysis of vertical axis wind turbines. Energy & Environment, 34 (7), 2815–2857. https://doi.org/10.1177/0958305x221121281
10. Tanasheva, N., Tleubergenova, A., Dyusembaeva, A., Satybaldin, A., Mussenova, E., Bakhtybekova, A. et al. (2023). Determination of the aerodynamic characteristics of a wind power plant with a vertical axis of rotation. Eastern-European Journal of Enterprise Technologies, 2 (8 (122)), 36–43. https://doi.org/10.15587/1729-4061.2023.277759
11. Kumar, R., Raahemifar, K., Fung, A. S. (2018). A critical review of vertical axis wind turbines for urban applications. Renewable and Sustainable Energy Reviews, 89, 281–291. https://doi.org/10.1016/j.rser.2018.03.033
12. Dewan, A., Gautam, A., Goyal, R. (2021). Savonius wind turbines: A review of recent advances in design and performance enhancements. Materials Today: Proceedings, 47, 2976–2983. https://doi.org/10.1016/j.matpr.2021.05.205
13. Pan, J., Ferreira, C., van Zuijlen, A. (2022). Estimation of power performances and flow characteristics for a Savonius rotor by vortex particle method. Wind Energy, 26 (1), 76–97. https://doi.org/10.1002/we.2788
14. Noman, A. A., Tasneem, Z., Sahed, Md. F., Muyeen, S. M., Das, S. K., Alam, F. (2022). Towards next generation Savonius wind turbine: Artificial intelligence in blade design trends and framework. Renewable and Sustainable Energy Reviews, 168, 112531. https://doi.org/10.1016/j.rser.2022.112531
15. Khudri Johari, M., Azim A Jalil, M., Faizal Mohd Shariff, M. (2018). Comparison of horizontal axis wind turbine (HAWT) and vertical axis wind turbine (VAWT). International Journal of Engineering & Technology, 7 (4.13), 74. https://doi.org/10.14419/ijet.v7i4.13.21333
16. Mohamed, O. S., Ibrahim, A. A., Etman, A. K., Abdelfatah, A. A., Elbaz, A. M. R. (2020). Numerical investigation of Darrieus wind turbine with slotted airfoil blades. Energy Conversion and Management: X, 5, 100026. https://doi.org/10.1016/j.ecmx.2019.100026
17. Yousefi Roshan, M., Khaleghinia, J., Eshagh Nimvari, M., Salarian, H. (2021). Performance improvement of Darrieus wind turbine using different cavity layouts. Energy Conversion and Management, 246, 114693. https://doi.org/10.1016/j.enconman.2021.114693
18. Tanasheva, N. K., Bakhtybekova, A. R., Shaimerdenova, K. M., Sakipova, S. E., Shuyushbayeva, N. N. (2022). Correction to: Modeling Aerodynamic Characteristics of a Wind Energy Installation with Rotating Cylinder Blades on the Basis of the Ansys Suite. Journal of Engineering Physics and Thermophysics, 95 (3), 846–846. https://doi.org/10.1007/s10891-022-02542-7
19. Tanasheva, N. K., Bakhtybekova, A. R., Shuyushbayeva, N. N., Tussupbekova, A. K., Tleubergenova, A. Zh. (2022). Calculation of the Aerodynamic Characteristics of a Wind-Power Plant with Blades in the Form of Rotating Cylinders. Technical Physics Letters, 48 (2), 51–54. https://doi.org/10.1134/s1063785022020092
20. Alassaf, O., Lukin, A., Demidova, G., Kozlov, G., Volkhontsev, A., Poliakov, N. (2022). Cylindrical Blades Magnus Wind Turbine Optimization and Control System. 2022 29th International Workshop on Electric Drives: Advances in Power Electronics for Electric Drives (IWED). https://doi.org/10.1109/iwed54598.2022.9722582
21. Al bkoor Alrawashdeh, K., Gharaibeh, N. S., Alshorman, A. A., Okour, M. H. (2021). Magnus Wind Turbine Effect Vertical Axis Using Rotating Cylinder Blades. JJMIE, 15 (2), 233–441. Available at: https://jjmie.hu.edu.jo/vol15-2/08-jjmie-48-19.pdf
22. Lukin, A., Demidova, G., Lukichev, D., Poliakov, N., Anuchin, A. (2023). Optimization of Cylindrical Blades for Wind Turbine Based on Magnus Effect. 2023 International Conference on Electromechanical and Energy Systems (SIELMEN). https://doi.org/10.1109/sielmen59038.2023.10290749
23. Dyusembaeva, A. N., Tleubergenova, A. Zh., Tanasheva, N. K., Nussupbekov, B. R., Bakhtybekova, A. R., Kyzdarbekova, Sh. S. (2023). Numerical investigation of the flow around a rotating cylinder with a plate under the subcritical regime of the Reynolds number. International Journal of Green Energy, 21 (5), 973–987. https://doi.org/10.1080/15435075.2023.2228394
24. Jeyan, J. V. M. L., Rupesh, A., Lal, J. (2018). Aerodynamic Shape Influence and Optimum Thickness Distribution Analysis of Perceptive Wind Turbine Blade. International Journal of Emerging Research in Management and Technology, 7 (3), 1. https://doi.org/10.23956/ijermt.v7i3.6
25. Prakoso, A. P., Warjito, W., Siswantara, A. I., Budiarso, B., Adanta, D. (2019). Comparison Between 6-DOF UDF and Moving Mesh Approaches in CFD Methods for Predicting Cross-Flow Pico- Hydro Turbine Performance. CFD Letters, 11 (6), 86–96. Available at: https://www.researchgate.net/publication/334446983_Com-

parison_Between_6-DOF_UDF_and_Moving_Mesh_Approaches_in_CFD_Methods_for_Predicting_Cross-Flow_Pico-_Hydro_Turbine_Performance

26. Yi, W., Bertin, C., Zhou, P., Mao, J., Zhong, S., Zhang, X. (2022). Aerodynamics of isolated cycling wheels using wind tunnel tests and computational fluid dynamics. Journal of Wind Engineering and Industrial Aerodynamics, 228, 105085. https://doi.org/10.1016/j.jweia.2022.105085
27. Liu, H., Yang, S., Tian, W., Zhao, M., Yuan, X., Xu, B. (2020). Vibration Reduction Strategy for Offshore Wind Turbines. Applied Sciences, 10 (17), 6091. https://doi.org/10.3390/app10176091

DOI: 10.15587/1729-4061.2024.299128

DEVELOPMENT OF A WIND TURBINE WITH TWO MULTIDIRECTIONAL WIND WHEELS (p. 47–57)

Sultanbek Issenov
S. Seifullin Kazakh Agrotechnical Research University, Astana, Republic of Kazakhstan
ORCID: https://orcid.org/0000-0003-4576-4621

Pyotr Antipov
QSM Resources LLP, Astana, Republic of Kazakhstan
ORCID: https://orcid.org/0009-0009-3667-8191

Marat Koshumbayev
S. Seifullin Kazakh Agrotechnical Research University, Astana, Republic of Kazakhstan
ORCID: https://orcid.org/0000-0002-2434-1905

Dauren Issabekov
Toraighyrov University, Pavlodar, Republic of Kazakhstan
ORCID: https://orcid.org/0000-0002-6673-5646

The object of research is a wind generator with counter-rotating blades. A special feature of this design is the presence of two wind wheels that rotate in opposite directions. Wind wheels are on the same axis, between them there is a certain distance, which is determined based on research data. The problem of modern wind power is the low range of operating wind speeds, weak generation at low wind speeds. The upper speed limit is 25 m/s, exceeding which leads to breakdowns of various units of the wind station, especially this affects the integrity of the blades, rupture of the wind wheel, cracking of the metal parts of the bearings and their fasteners. The wind turbine presented in the article allows to achieve an increase in the generation of electric energy by 50–70 %. This is achieved by increasing the relative rotational speed of the rotor relative to the stator. Therefore, even at low speeds, the rotor speed relative to the stator increases, which leads to an increase in power generation. The design of the device includes: two wind wheels, one transmits its rotation to the stator, the second to the rotor axis, a metal base, a current collector mechanism. For conducting the research, an experimental model and a semi-industrial installation were used. Results studies have confirmed the theoretical increase in the generation of electrical energy by this design. The peculiarity of the obtained results is connected with the determination of the distance between two wind wheels, the optimal distance between them corresponds to the maximum energy generation. A distinctive feature of the results obtained can be considered an increase in the number of blades on the second wind wheel.

Keywords: wind device, multidirectional wind wheels, gap, blades, model, wind speed.

References

1. Korobatov, D. V., Kozlov, S. V., Sirotkin, E. A. (2016). Historic and economic analysis of wind turbines and control systems. Alternative Energy and Ecology (ISJAEE), 15-18, 54–66. https://doi.org/10.15518/isjaee.2016.15-18.054-066
2. Koshumbaev, M., Issenov, S., Iskakov, R., Bulatbayeva, Y. (2023). Development of a vortex wind device. Eastern-European Journal of Enterprise Technologies, 1 (8 (121)), 22–29. https://doi.org/10.15587/1729-4061.2023.274199
3. Kaidar, A., Issenov, S., Sheryazov, S., Kislov, A., Antipov, P. (2022). Overview of wind turbine systems. The International Scientific Conference «22nd Satbayev Readings». Pavlodar, 169–180.
4. Moghadassian, B., Rosenberg, A., Sharma, A. (2016). Numerical Investigation of Aerodynamic Performance and Loads of a Novel Dual Rotor Wind Turbine. Energies, 9 (7), 571. https://doi.org/10.3390/en9070571
5. Rosenberg, A., Selvaraj, S., Sharma, A. (2014). A Novel Dual-Rotor Turbine for Increased Wind Energy Capture. Journal of Physics: Conference Series, 524, 012078. https://doi.org/10.1088/1742-6596/524/1/012078
6. Pustynnikov, S. V. (2011). Pat. No. RU 2429375 C1. Two-rotor solenoid wind generator.
7. Kaidar, A. B., Shapkenov, B. K., Kislov, A. P., Markovsky, V. P. (2015). New windwheels with improved energy indicators. Bulletin of PSU ENERGY series, 2, 46–52. Available at: https://vestnik-energy.tou.edu.kz/storage/journals/104.pdf
8. Kaidar, A. B., Shapkenov, B. K., Issenov, S. S., Sheryazov, S. K., Antipov, P. A., Shishkin, A. V. (2023). Pat. No. 36163 KZ. Autonomous power supply system with controlled starting moment of the wind wheel. No. 2022/0073.
9. Chen, J., Yin, F., Li, X., Ye, Z., Tang, W., Shen, X., Guo, X. (2022). Unsteady aerodynamic modelling for dual-rotor wind turbines with lifting surface method and free wake model. Journal of Physics: Conference Series, 2265 (4), 042055. https://doi.org/10.1088/1742-6596/2265/4/042055
10. Koehuan, V. A., Sugiyono, Kamal, S. (2017). Investigation of Counter-Rotating Wind Turbine Performance using Computational Fluid Dynamics Simulation. IOP Conference Series: Materials Science and Engineering, 267, 012034. https://doi.org/10.1088/1757-899x/267/1/012034
11. Ozbay, A., Tian, W., Hu, H. (2015). An Experimental Investigation on the Wake Characteristics and Aeromechanics of Dual-Rotor Wind Turbines. Volume 9: Oil and Gas Applications; Supercritical CO_2 Power Cycles; Wind Energy. https://doi.org/10.1115/gt2015-43805
12. Lee, S., Kim, H., Lee, S. (2010). Analysis of aerodynamic characteristics on a counter-rotating wind turbine. Current Applied Physics, 10 (2), S339–S342. https://doi.org/10.1016/j.cap.2009.11.073

13. Maduka, M., Li, C. W. (2022). Experimental evaluation of power performance and wake characteristics of twin flanged duct turbines in tandem under bi-directional tidal flows. Renewable Energy, 199, 1543–1567. https://doi.org/10.1016/j.renene.2022.09.067
14. Erturk, E., Sivrioglu, S., Bolat, F. C. (2018). Analysis Model of a Small Scale Counter-Rotating Dual Rotor Wind Turbine with Double Rotational Generator Armature. International Journal of Renewable Energy Research, v8i4. https://doi.org/10.20508/ijrer.v8i4.8235.g7549

DOI: 10.15587/1729-4061.2024.297541

DEVELOPMENT OF A NEW FAST DRYING DETERMINANT METHOD USING RESISTIVITY FOR THE INDUSTRY OF COCONUT SHELL CHARCOAL BRIQUETTES (p. 58–66)

Andreas Prasetyadi
Sanata Dharma University, Sleman, Indonesia
ORCID: https://orcid.org/0000-0002-6235-597X

Rusdi Sambada
Sanata Dharma University, Sleman, Indonesia
ORCID: https://orcid.org/0000-0002-6555-7307

Petrus Kanisius Purwadi
Sanata Dharma University, Sleman, Indonesia
ORCID: https://orcid.org/0009-0000-1094-9672

The charcoal briquette industry faces the problem of the method for determining the drying stop during its production. The combustion method as the main method is time-consuming. The test needs 3 hours to get the result. In order to find a new fast method for drying determinant, the resistivity method was proposed for rainbow coconut shell charcoal briquettes. The briquettes had a length of 3.8 cm, height of 2.2 cm, and width of 2 cm with a half-tubular top side. 50 samples of each three drying conditions (wet, half-dry, and dry) of the same drying batch were collected. These conditions were determined by a drying expert of a coconut shell charcoal briquette company. Then, the resistances were measured and the geometrical factor was applied to find their resistivities. A model of resistivity in the cross-sectional layer was also applied to find the coefficients of front-tail, base-top, and side-side directions. These coefficients became a special way to find the position of the wet part in half-dry briquettes. The results of the work show that resistivities in combination with their distribution can potentially be used for fast drying stop determinant. The wet and dry briquettes have a resistivity difference order of 10^2. The resistivities of the wet and dry briquettes are 450 kiloohms and 28 megaohms for every centimeter of length, respectively. The half-dry and dry briquettes have the same order of resistivities. However, the resistivity distribution of both conditions is very different. The dry briquettes have homogenous resistivities among the measurements emphasizing the drying process of the solid. It was also found that the half-dry briquette has a surface dry part until 0.55 cm depth. The center of the briquette is still wet.

Keywords: charcoal briquette, resistance measurement, fast drying determinant, resistivity method.

References

1. Łaska, G., Ige, A. R. (2023). A Review: Assessment of Domestic Solid Fuel Sources in Nigeria. Energies, 16 (12), 4722. https://doi.org/10.3390/en16124722
2. Khan, A. U., Jan, Q. M. U., Abas, M., Muhammad, K., Ali, Q. M., Zimon, D. (2023). Utilization of Biowaste for Sustainable Production of Coal Briquettes. Energies, 16 (20), 7025. https://doi.org/10.3390/en16207025
3. Marreiro, H. M. P., Peruchi, R. S., Lopes, R. M. B. P., Andersen, S. L. F., Eliziário, S. A., Rotella Junior, P. (2021). Empirical Studies on Biomass Briquette Production: A Literature Review. Energies, 14 (24), 8320. https://doi.org/10.3390/en14248320
4. Sunardi, S., Djuanda, D., Mandra, M. A. S. (2019). Characteristics of Charcoal Briquettes from Agricultural Waste with Compaction Pressure and Particle Size Variation as Alternative Fuel. International Energy Journal, 19 (3), 139–148. Available at: http://www.rericjournal.ait.ac.th/index.php/reric/article/view/2199
5. Doloksaribu, M. (2014). Pembuatan Briket Arang Dari Tanah Gambut Pengganti Kayu Bakar. Jurnal Pengabdian kepada masyarakat Penerapan Ipteks, 20 (75), 70–77. Available at: https://www.researchgate.net/publication/314080916_Pembuatan_Briket_Arang_Dari_Tanah_Gambut_Pengganti_Kayu_Bakar
6. Adam, S. N. F. S., Aiman, J. H. M., Zainuddin, F., Hamdan, Y. (2021). Processing and Characterisation of Charcoal Briquettes Made from Waste Rice Straw as A Renewable Energy Alternative. Journal of Physics: Conference Series, 2080 (1), 012014. https://doi.org/10.1088/1742-6596/2080/1/012014
7. Osei Bonsu, B., Takase, M., Mantey, J. (2020). Preparation of charcoal briquette from palm kernel shells: case study in Ghana. Heliyon, 6 (10), e05266. https://doi.org/10.1016/j.heliyon.2020.e05266
8. Lestari, L., Variani, V. I., Firihu, Muh. Z., Raharjo, S., Saleh, I., Aprilla, N. (2020). Effect of Compaction Pressure on Quality of Activated Charcoal Briquette Made from Sago Stem Midrib Material. IOP Conference Series: Materials Science and Engineering, 797 (1), 012022. https://doi.org/10.1088/1757-899x/797/1/012022
9. Hamzah, F., Fajri, A., Harun, N., Pramana, A. (2023). Characterization of charcoal briquettes made from rubber rods and coconut shells with tapioca as an adhesive. IOP Conference Series: Earth and Environmental Science, 1182 (1), 012071. https://doi.org/10.1088/1755-1315/1182/1/012071
10. Jarawi, N., Jusoh, I. (2023). Charcoal properties of Malaysian bamboo charcoal carbonized at 750 °C. BioResources, 18 (3), 4413–4429. https://doi.org/10.15376/biores.18.3.4413-4429
11. Kwon, S.-M., Kwon, G.-J., Jang, J.-H., Kim, N.-H. (2012). Characteristics of Charcoal in Different Carbonization Temperatures. Journal of Forest and Environmental Science, 28 (4), 263–267. https://doi.org/10.7747/jfs.2012.28.4.263
12. Yan, W., Chen, Z., Sheng, K. (2015). Carbonization temperature and time improving quality of charcoal briquettes. Transactions of the Chinese Society of Agricultural Engineering, 31 (24), 245–249. doi: https://doi.org/10.11975/j.issn.1002-6819.2015.24.037
13. Saneewongnaayutaya, N., Khamdaeng, T., Panyoyai, N., Tippayawong, N., Wongsiriamnuay, T. (2022). Production and characterization of fuel briquettes from rice husks and tobacco stalks. AIP Conference Proceedings. https://doi.org/10.1063/5.0115139

14. Njenga, M. et al. (2021). Challenges and opportunities for charcoal briquette enterprises in East Africa. Available at: https://www.researchgate.net/publication/352561574_Challenges_and_opportunities_for_charcoal_briquette_enterprises_in_East_Africa
15. Adam, S. N. F. S., Zainuddin, F., Morgan, N. Z. S., Saroni, H. H. (2023). Comparison of Corn and Tapioca Starch Binders on the Characteristic of Rice Straw Charcoal Briquettes. Emerging Technologies for Future Sustainability, 59–69. https://doi.org/10.1007/978-981-99-1695-5_5
16. Pratama, B. H., Syarief, A., Saputra, M. R. P., Azis, A. P. (2022). Effect of Compaction Pressure and Sawdust Size on Briquette Made from Ulin Wood (Eusideroxylon Zwageri) and Gelam Wood (Melaleuca Cajuputi) to Combustion Characteristics. International Journal of Mechanical Engineering Technologies and Applications, 3 (2), 100. https://doi.org/10.21776/mechta.2022.003.02.4
17. Rapheal, I. A., Abayomi, B. (2021). Production and Characterisation of Briquettes from Maize Stalk and Neem Leaves Admixture. Acta Chemica Malaysia (ACMY), 5 (2), 77–81. Available at: https://www.actachemicamalaysia.com/acmy-02-2021-77-81/
18. Mencarelli, A., Cavalli, R., Greco, R. (2022). Variability on the energy properties of charcoal and charcoal briquettes for barbecue. Heliyon, 8 (8), e10052. https://doi.org/10.1016/j.heliyon.2022.e10052
19. Grover, P. D., Mishra, S. K. (1996). Biomass briquetting: Technology and Practices. Regional Wood Energy Development in Asia. Field Document No. 46. Food and Agriculture Organization of the United Nations. Bangkok. Available at: https://leehite.org/biomass/documents/Biomass%20Briquetting%20Technology%20and%20Practices%20FAO.pdf
20. Parikh, D. M. (2014). Solids Drying: Basics and Applications. Chemical Engineering, 42–45. Available at: https://www.researchgate.net/publication/283088778_Solids_Drying_Basics_and_Applications
21. Song, X., Wei, J., Mao, Z., Chi, X., Zhu, Z., Han, G., Cheng, W. (2023). Effect of Hot-Air Drying Conditions on the Drying Efficiency and Performance of a Waterborne Coating on Pine Wood. Forests, 14 (9), 1752. https://doi.org/10.3390/f14091752
22. Paul, G., Olivier, M., Esther, A., Daniel, M., Jean, C.-L. (2019). Heat and Mass Transfer Local Modelling Applied to Biomass Briquette Drying. Procedia Manufacturing, 35, 149–154. https://doi.org/10.1016/j.promfg.2019.05.018
23. Brennan, J. K., Bandosz, T. J., Thomson, K. T., Gubbins, K. E. (2001). Water in porous carbons. Colloids and Surfaces A: Physicochemical and Engineering Aspects, 187-188, 539–568. https://doi.org/10.1016/s0927-7757(01)00644-6
24. Rembert, F., Jougnot, D., Guarracino, L. (2020). A fractal model for the electrical conductivity of water-saturated porous media during mineral precipitation-dissolution processes. Advances in Water Resources, 145, 103742. https://doi.org/10.1016/j.advwatres.2020.103742
25. Ibrahim, M. H. I., Said, M. N., Asmawi, R. (2015). Characterization of Carbon Brush from Coconut Shell for Railway Application. Applied Mechanics and Materials, 773-774, 291–295. https://doi.org/10.4028/www.scientific.net/amm.773-774.291
26. Gunawan, S., Nursanni, B., Suprapto, Januariyansah, S. (2022). The utilization of biomass waste as charcoal briquette to reduce waste disposal. Journal of Physics: Conference Series, 2193 (1), 012086. https://doi.org/10.1088/1742-6596/2193/1/012086

АНОТАЦІЇ

ENERGY-SAVING TECHNOLOGIES AND EQUIPMENT

DOI: 10.15587/1729-4061.2024.298202

ПОРІВНЯЛЬНИЙ АНАЛІЗ ШВИДКОГО ГАЗООХОЛОДЖУВАНОГО РЕАКТОРА З ВИКОРИСТАННЯМ ГЕТЕРОГЕННИХ КОНФІГУРАЦІЙ АКТИВНОЇ ЗОНИ З ТРЬОМА І П'ЯТЬМА ВАРІАНТАМИ ПАЛИВА (с. 6–17)

Fajri Prasetya, Ratna Dewi Syarifah, Iklimatul Karomah, Indarta Kuncoro Aji, Nuri Trianti

GFR або швидкий газоохолоджуваний реактор є одним із видів швидких реакторів IV покоління, в якому використовується дуже висока температура охолодження. Таким чином, для того, щоб розподіл потужності утворюваних нейтронів досягав безпечної та рівномірної граничної точки необхідна правильна конструкція активної зони реактора. Використання однорідної (гомогенної) активної зони реактора може дати пікову потужність. Цього можна уникнути, оскільки це призведе до аварії реактора. У даній роботі дослідники спробували порівняти результати аналізу двох гетерогенних конструкцій активної зони реактора, включаючи конфігурацію з 3 варіантами палива і 5 варіантами палива з використанням палива UN-PuN. Метою дослідження є визначення величини k_{eff}, одержуваної при обох типах варіантів палива протягом 5 років вигорання, а також визначення характеристик потоку нейтронів, швидкості ділення та продуктів ділення протягом 15 років вигорання. На початку дослідження було розраховано гомогенну та гетерогенну активні зони з 3 та 5 варіантами палива з моделюванням переносу нейтронів з використанням OpenMC. Результати розрахунків показують, що гетерогенна конфігурація активної зони з 5 варіантами палива за значенням k_{eff} є оптимальною в порівнянні з 3 варіантами палива, оскільки вона має найменше значення надлишкової реактивності. Характеристики потоку нейтронів та швидкості поділу для 5 варіантів палива мають більш рівномірний розподіл у порівнянні з 3 варіантами палива, що забезпечує підтримку часу життя нейтронів та терміну служби реактора. Залишковий плутонієвий матеріал вигорання та незначні актинідні відходи для 5 варіантів палива мають меншу масу, ніж для 3 варіантів палива. Реактори типу GFR з гетерогенними конструкціями активної зони для 5 варіантів палива мають більш високі результати нейтронного аналізу з точки зору критичності реактора, розподілу потужності нейтронів та утворення відходів. Зрештою, оптимізація об'ємної частки палива UN-PuN на рівні 60 % забезпечує оптимальне значення k_{eff}.

Ключові слова: порівняльний, варіанти палива, швидкий газоохолоджуваний реактор, гетерогенний, k_{eff}, активна зона реактора.

DOI: 10.15587/1729-4061.2024.290996

НЕЙТРОННА КОНСТРУКЦІЯ МАЛОГО МОДУЛЬНОГО ВОДЯНОГО РЕАКТОРА ПІД ТИСКОМ НА КАРБІДНОМУ ПАЛИВІ ТОРІЮ НА РІВНІ ПОТУЖНОСТІ 300–500 МВт (с. 18–27)

Boni Pahlanop Lapanporo, Zaki Su'ud, Asril Pramutadi Andi Mustari

У цьому дослідженні представлено нейтронну конструкцію невеликого модульного реактора з водою під тиском (МВТ) з тривалим терміном служби, на якому використовується паливо з карбіду торію з розщеплюваним матеріалом ^{233}U. Цільовою оптимізацією для цього дослідження є реактор, розрахований на роботу протягом 20 років, з надлишковою реактивністю протягом усього робочого циклу реактора постійно нижче 1,00 % dk/k. Аналіз передбачає поділ активної зони реактора на три паливні області з рівнями збагачення ^{233}U в діапазоні від 3 % до 8 %, з різницею в 1 % для кожної паливної області. Щоб досягти оптимальних умов, до палива довільно додавали 231 Па. Об'ємна частка палива в цій конструкції змінювалася від 30 % до 65 % із зміною на 5 %. Варіації рівня потужності також досліджувалися в межах 300–500 МВт з кроком 50 МВт. Розрахунки проводилися за допомогою програми Standard Reactor Analysis Code (SRAC) з модулями PIJ і CITATION для розрахунків клітин і керна з використанням нуклідних даних JENDL-4.0. Нейтронні розрахунки показують, що паливо з об'ємною часткою 60 % досягає оптимальних умов на рівні потужності 300 МВт·год. Найкращі показники спостерігалися з об'ємною часткою палива 65 %, досягаючи оптимальних умов на рівнях потужності від 300 до 500 МВт·год. Для палива з найкращими характеристиками розподіл щільності потужності для низьких і високих рівнів потужності відповідає тій самій моделі радіально та аксіально. Піковий коефіцієнт потужності (ПКП) для всіх конфігурацій палива, що наближаються до оптимальних умов, залишається нижче двох, що є безпечною межею для ПКП. Інші параметри нейтронної безпеки, такі як коефіцієнт Доплера та коефіцієнт пористої фракції, також залишаються в безпечних межах для ПКП, при цьому обидва значення залишаються від'ємними протягом усього робочого циклу реактора.

Ключові слова: торій, конструкція сердечника, доплерівська реактивність, коефіцієнт пористості, CITATION.

DOI: 10.15587/1729-4061.2024.298915

УДОСКОНАЛЕННЯ МОДЕЛІ РОТОРА САВОНІУСА ДОДАТКОВИМИ КАНАВКАМИ ДЛЯ ПІДВИЩЕННЯ ПРОДУКТИВНОСТІ ГІДРОКІНЕТИЧНОЇ ТУРБІНИ (с. 28–37)

Petrus Sampelawang, Nasaruddin Salam, Luther Sule, Rustan Tarakka

У гідрокінетичних турбінах використовуються різні ротори з технологічних та економічних причин. Незважаючи на низьку продуктивність, у гідрокінетичних турбінах із вертикальною віссю використовується ротор Савоніуса. Об'єктом дослідження є модель ротора Савоніуса з додатковими канавками. У дослідженні розглядається необхідність підвищення ККД та загальної

продуктивності моделей роторів Савоніуса в гідрокінетичних турбінах, які широко застосовуються для використання енергії поточних водних потоків. Задача полягає у розумінні того, як різні конфігурації канавок впливають на аеродинамічні характеристики та ефективність вилучення енергії ротора Савоніуса в гідрокінетичних турбінах. Результати випробувань показали, що додавання канавок призвело до помітного підвищення ККД (η) та коефіцієнта опору (CD). Лопатки з канавками показали максимальний ККД 30,97 % та максимальний коефіцієнт лобового опору 2,71. Примітно, що оптимальною моделлю виявилися лопатки з шириною канавки 12,5 мм, що продемонстрували максимальний ККД 35,66 % та коефіцієнт лобового опору 3,08. Це свідчить про суттєве підвищення ККД на 4,69 % та відповідне збільшення коефіцієнта лобового опору на 0,37 для лопаток з канавками. Канавки на рифлених лопатках збільшують тертя, покращуючи продуктивність. Лопатки ротора з канавками значно покращують продуктивність турбіни. Моделі роторів Савоніуса в гідрокінетичних турбінах дозволяють вилучити більше енергії за рахунок оптимізації ширини та розташування канавок для максимального підвищення коефіцієнта лобового опору та ККД. Дослідження стосується проектування та оптимізації гідрокінетичних турбін для виробництва відновлюваної енергії. Із застосуванням результатів даного дослідження інженери та проектувальники можуть покращити продуктивність та ККД моделі ротора Савоніуса в гідрокінетичних турбінах.

Ключові слова: гідрокінетична турбіна, ротор Савоніуса, лопатка з канавками, коефіцієнт лобового опору, відносна швидкість гвинта.

DOI: 10.15587/1729-4061.2024.298599

ВИЯВЛЕННЯ ДЕЯКИХ ЗАКОНОМІРНОСТЕЙ АЕРОДИНАМІКИ НАВКОЛО ВІТРОВИХ ТУРБІН З ВЕРТИКАЛЬНОЮ ВІССЮ ОБЕРТАННЯ (с. 38–46)

Nazgul Tanasheva, Gulden Ranova, Amangeldy Satybaldin, Ainura Dyusembaeva, Asem Bakhtybekova, Nurgul Shuyushbayeva, Sholpan Kyzdarbekova, Indira Sarzhanova, Nurgul Abdirova

Конструкція вітряних турбін з вертикальною віссю обертання досить проста, що успішно підвищує рівень ККД. Існуючі лопатеві вітрові турбіни мають відсутність струмів у вигляді негативного крутного моменту, а установки, що працюють на ефекті Магнуса, мають низький підйом. У зв'язку з цим розробка і дослідження установок, що працюють на швидкостях від 3 м/сек, з комбінованими лопатями з підвищеною ефективністю роботи, є актуальною темою.

Об'єктом дослідження є вітряна турбіна, що складається з системи обертових циліндрів і нерухомих лопатей, що працюють при низьких швидкостях повітряного потоку, починаючи з 3 м/с. Чисельні дослідження проводилися з використанням програми Ansys Fluent і реалізованої моделі турбулентності *k*-ε. Особливістю роботи є комбіноване використання двох підйомних сил: циліндра і нерухомих лопатей, що дозволило збільшити вихідні аеродинамічні параметри. Розрахунки були виконані для швидкостей вхідного потоку 3 м/сек, 9 м/сек, 15 м/сек і швидкостей обертання циліндра 315 об/хв, 550 об/хв, 720 об/хв.визначено, що період зміни моменту сил *T* становить 0,5 м/сек, що відповідає 2 оборотам вітроколеса в хвилину. Було встановлено, що частота обертання циліндра в діапазоні від 315 об/хв до 720 об/хв не впливає на період зміни моменту сил, але амплітуда моменту сил збільшується зі зменшенням частоти обертання. Також отримані залежності швидкості обертання вітроколеса від швидкості набігаючого потоку, знайдені методом ковзних сіток і 6DOF. Визначено, що установка починає здійснювати обороти від 3 м/с, при позитивному крутному моменті сил. Область практичного застосування чисельних результатів буде корисною для подальших досліджень комбінованих вітрових турбін.

Ключові слова: комбінована лопать, фіксована лопать, Ansys-Fluent, момент сил.

DOI: 10.15587/1729-4061.2024.299128

РОЗРОБКА ВІТРОВОЇ ТУРБІНИ З ДВОМА РІЗНОНАПРАВЛЕНИМИ ВІТРОВИМИ КОЛЕСАМИ (с. 47–57)

Sultanbek Issenov, Pyotr Antipov, Marat Koshumbayev, Dauren Issabekov

Об'єктом дослідження є вітрогенератор із зустрічно обертовими лопатями. Особливістю такої конструкції є наявність двох вітрових коліс, які обертаються в протилежних напрямках. Вітрові колеса знаходяться на одній осі, між ними є певна відстань, яка визначається на основі даних досліджень. Проблемою сучасної вітроенергетики є низький діапазон робочих швидкостей вітру, слабка генерація при малих швидкостях вітру. Верхня межа швидкості становить 25 м/с, перевищення якої призводить до поломок різних вузлів вітрової станції, особливо це позначається на цілісності лопатей, розриві вітрового колеса, розтріскування металевих частин підшипників та їх кріплень. Представлений у статті вітрогенератор дозволяє досягти збільшення вироблення електроенергії на 50–70 %. Це досягається збільшенням відносної швидкості обертання ротора відносно статора. Тому навіть при низьких швидкостях обертання ротора відносно статора зростає, що призводить до збільшення вироблення електроенергії. У конструкцію пристрою входять: два вітрових колеса, одне передає своє обертання на статор, друге на вісь ротора, металева основа, струмоприймальний механізм. Для проведення досліджень використовували експериментальний макет і напівпромислову установку. Результати досліджень підтвердили теоретичне збільшення генерації електроенергії цією конструкцією. Особливість отриманих результатів пов'язана з визначенням відстані між двома вітровими колесами, оптимальна відстань між якими відповідає максимальному виробленню енергії. Відмінною особливістю отриманих результатів можна вважати збільшення кількості лопатей на другому вітровому колесі.

Ключові слова: вітровий пристрій, різноспрямовані вітрові колеса, зазор, лопаті, модель, швидкість вітру.

DOI: 10.15587/1729-4061.2024.297541

РОЗРОБКА НОВОГО ШВИДКОГО МЕТОДУ ВИЗНАЧЕННЯ ВИСИХАННЯ З ВИКОРИСТАННЯМ ПИТОМОГО ОПОРУ ДЛЯ ВИРОБНИЦТВА БРИКЕТІВ З КОКОСОВОГО ВУГІЛЛЯ (с. 58–66)

Andreas Prasetyadi, Rusdi Sambada, Petrus Kanisius Purwadi

Виробництво деревновугільних брикетів стикається з проблемою методу визначення зупинки сушіння у процесі їх виготовлення. Спалювання в якості основного методу є трудомістким. Отримання результату випробування займає 3 години. Для знаходження нового швидкого методу визначення висихання був запропонований метод питомого опору для брикетів з райдужного кокосового вугілля. Брикети мали довжину 3,8 см, висоту 2,2 см і ширину 2 см з напівтрубчастою верхньою стороною. З однієї і тієї ж партії сушіння було відібрано 50 зразків для кожного з трьох ступенів висихання (вологий, напівсухий і сухий). Ці ступені були визначені спеціалістом із сушіння підприємства з виробництва брикетів з кокосового вугілля. Потім були виміряні опори та застосований геометричний коефіцієнт для визначення їх питомого опору. Також була застосована модель питомого опору в шарі поперечного перерізу для знаходження коефіцієнтів напрямків перед-зад, основа-верх та бік-бік. Ці коефіцієнти стали особливим способом визначення положення вологої частини в напівсухих брикетах. Результати роботи показують, що питомі опори в поєднанні з їх розподілом потенційно можуть бути використані для швидкого визначення зупинки сушіння. Різниця у питомому опорі вологих та сухих брикетів становить порядку 102. Питомий опір вологих та сухих брикетів становить 450 кілоом та 28 мегаом на кожен сантиметр довжини відповідно. Напівсухі та сухі брикети мають однаковий порядок питомого опору. Однак розподіл питомого опору в обох умовах сильно відрізняється. Сухі брикети мають однорідний питомий опір за вимірами, що підкреслює процес сушіння твердої речовини. Також було виявлено, що напівсухий брикет має суху частину поверхні глибиною до 0,55 см. Середина брикету все ще залишається вологою.

Ключові слова: деревновугільний брикет, вимірювання опору, швидке визначення висихання, метод питомого опору.